

# Threshold-Dependence Study for Narrow-pitch-strip CMS RPCs

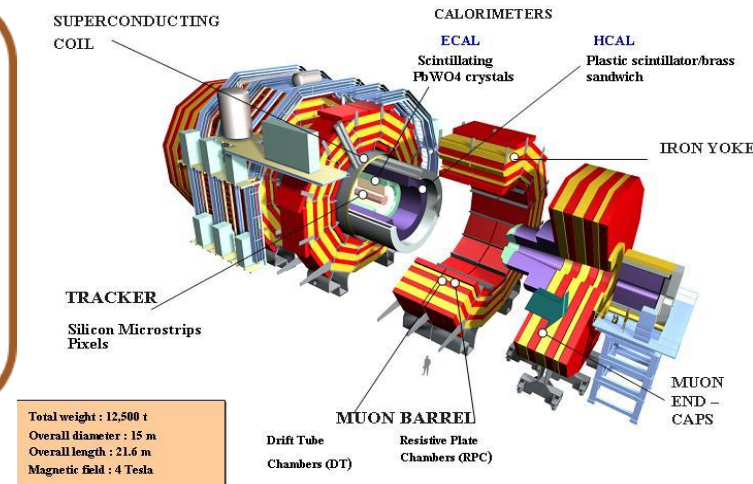
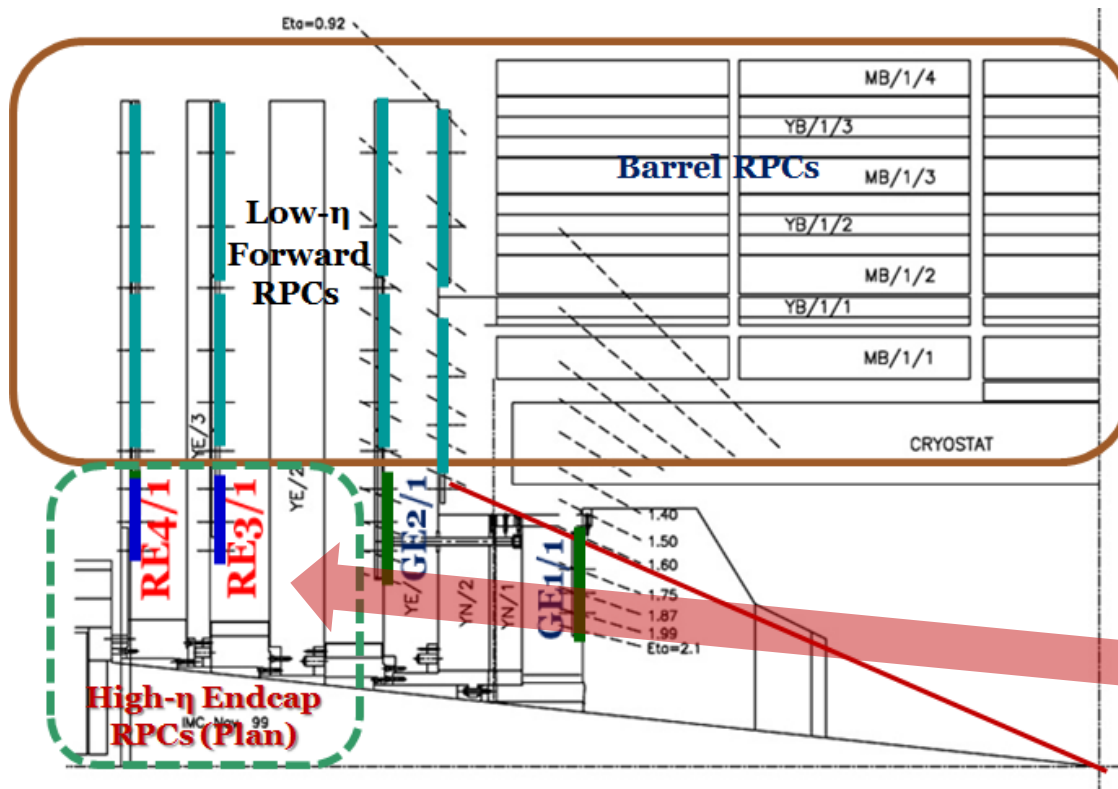
*Kyong Sei Lee, KODEL, Korea University*  
*On Behalf of the CMS RPC Collaboration*

1. Motivation
2. Test of the prototype RPCs at KODEL and GIF++/CERN
3. Conclusions

# 1. Motivation

The present detector R&D is for future CMS RPCs at high backgrounds

- ✓ In the current CMS muon system, Barrel + 4 endcap RPC stations (+ & -) composed of double-gap RPCs in  $|\eta| < 1.6$
- ✓ In the PHASE I upgrade, 4<sup>th</sup> RPC station in  $|\eta| < 1.6$  has been completed in 2014.
- ✓ In the PHASE II upgrade by 2023, new endcap RPCs in  $1.6 < |\eta| < 2.1(2.4)$  are currently proposed.



**RPCs in high- $\eta$  to be developed in the phase II upgrade**

## Direction of R & Ds for the high- $\eta$ CMS RPCs (at RE3/1 and RE4/1)

We have pursued **better detector performance** ensuring higher rate capability for the future CMS RPCs:

- ✓ More sensitive detectors and electronics
  - Better for reducing the probability of aging due to high-rate background
  - **To guarantee the better longevity of the RPC gaps**
- ✓ Lower resistivity → **Rate capability  $\sim 1/\rho$**

### Resistive plates for CMS RPCs

- ✓ HPL (high pressurized laminate):  $\rho \sim \text{a few } 10^{10} \Omega \text{ cm}$ 
  - Still, the best choice in virtue of the low unit price.

**In the present R&D, two different type RPCs have been suggested and tested at GIF++/H4 and KODEL/KU.**

**Type A: two 1.6-mm-thick (instead of 2.0-mm thickness) double-gap RPCs**

Effective HV = 7.8 ~ 8.4 kV (15% lower compare to that of the current CMS RPCs)

**Type B: two 0.8-mm-thick four-gap (multi-gap) RPCs**

Effective HV = 9.0 ~ 9.8 kV (~ same with that of the current CMS RPCs)

**Advantage** → **The detector current induced by high-rate particles is four times lower.**

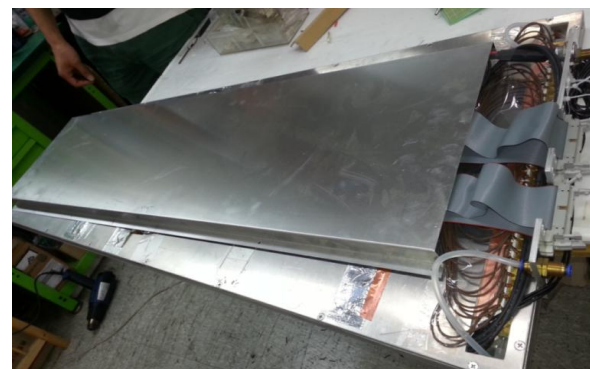
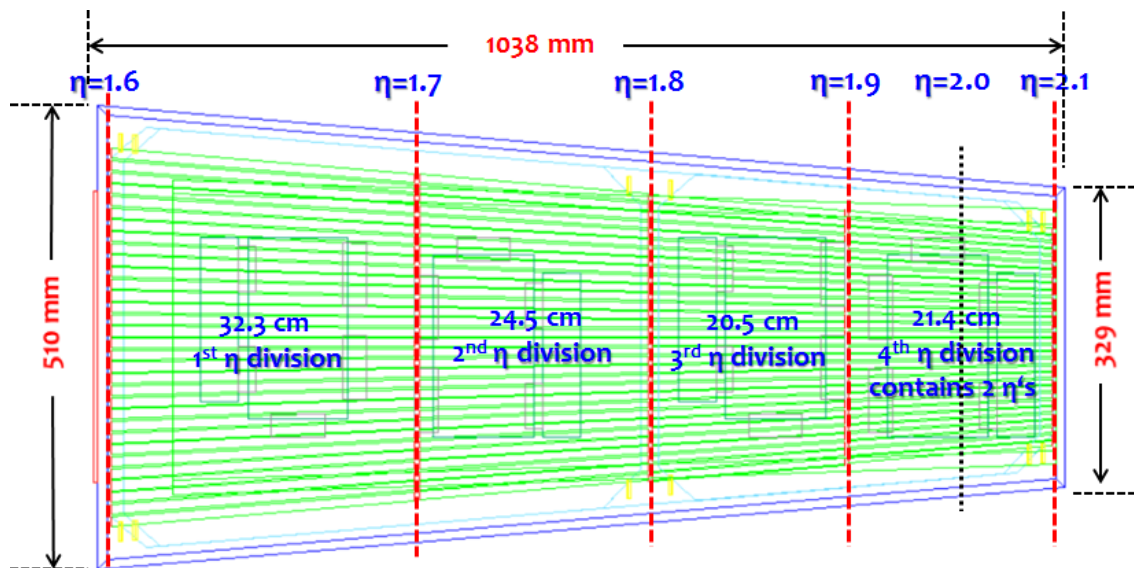
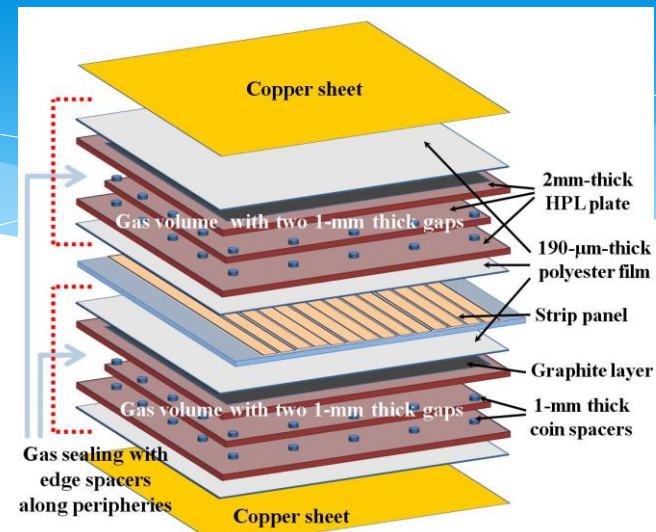
# Prototype RPCs tested at GIF++ and KODEL

Have chosen the old RE1/1 RPC geometry (10°)

~ an half size of RE3/1 or RE4/1 (20°)

Strip lengths & pitches are close to RE3/1 (RE4/1).

- ✓ **Narrow-pitch and short strips**
- ✓ Strip pitches: 7.5 ~ 13.3 mm
- ✓ Strip length: 32.3 cm (1.6~1.7) / 24.5 cm (1.7~1.8) / 20.5 cm (1.8~1.9) / 21.4 cm (1.9~2.1)





## Two different type front-end electronics

1. 32-ch FEBs currently used for the CMS RPC operation
2. New 32-ch FEBs manufactured with commercial preamplifiers (voltage sensitive)
  - ✓ Input impedance =  $20 \Omega$
  - ✓ Gain = 200 mV/mV
  - ✓ Ethernet communication for adjusting thresholds
  - ✓ LVDS output pulse width = 70 ns (fixed)
  - ✓ Minimum sensitivity  $\sim 0.1$  mV ( $\sim 20$  fC)
  - ✓ Time resolution  $\sim 200$  ps



### For double-gap RPCs,

| New FEBs     | CMS RPC FEBs     |
|--------------|------------------|
| Th = 1.0 mV  | Th $\sim 180$ fC |
| Th = 0.75 mV | Th $\sim 135$ fC |
| Th = 0.60 mV | Th $\sim 110$ fC |

Equivalent

### For multi-gap (4-gap) RPCs,

| New FEBs     | CMS RPC FEBs     |
|--------------|------------------|
| Th = 1.0 mV  | Th $\sim 120$ fC |
| Th = 0.75 mV | Th $\sim 90$ fC  |
| Th = 0.60 mV | Th $\sim 70$ fC  |

Equivalent

## 2. Test of the prototype RPCs at KODEL and GIF++/CERN

200-mCi  $^{137}\text{Cs}$  at KODEL/Korea University.

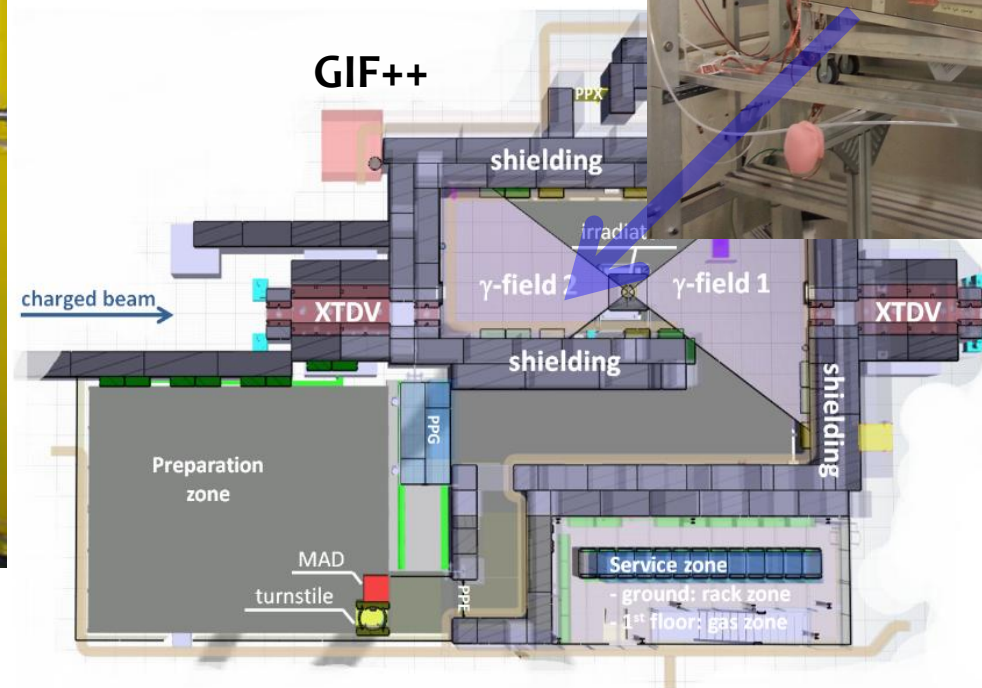
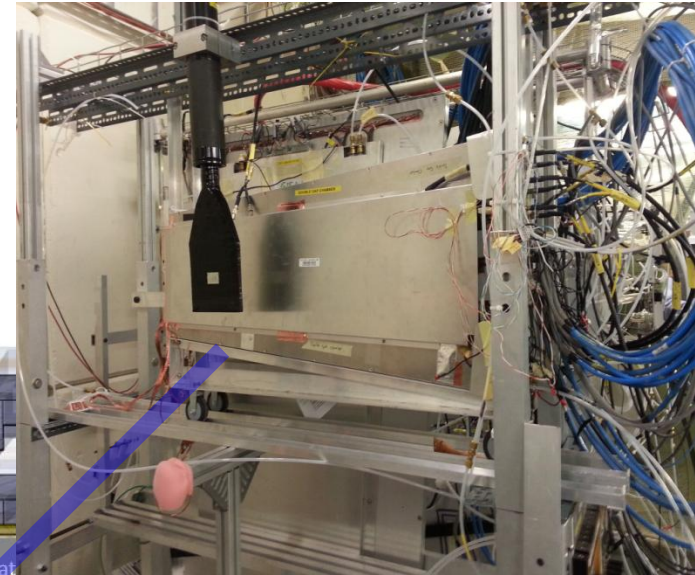
Current activity = 5.55 GBq

Maximum  $\gamma$  rate at 37 cm  $\sim 1.4 \text{ kHz cm}^{-2}$

GIF++ installed at H4 beam line

Activity = 1.4 TBq ( $^{137}\text{Cs}$ )

Maximum  $\gamma$  rate at the test position  $\sim 1.5 \text{ kHz cm}^{-2}$



## Realized a strong strip-pitch dependence of the RPC data

Checked threshold dependences of efficiencies & mean cluster sizes

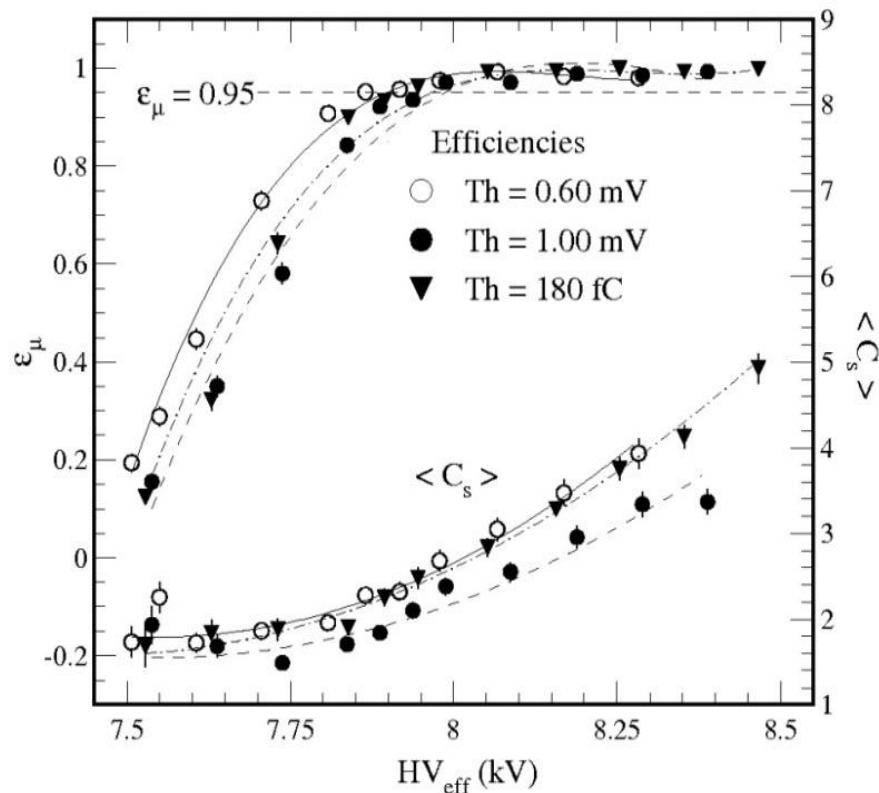
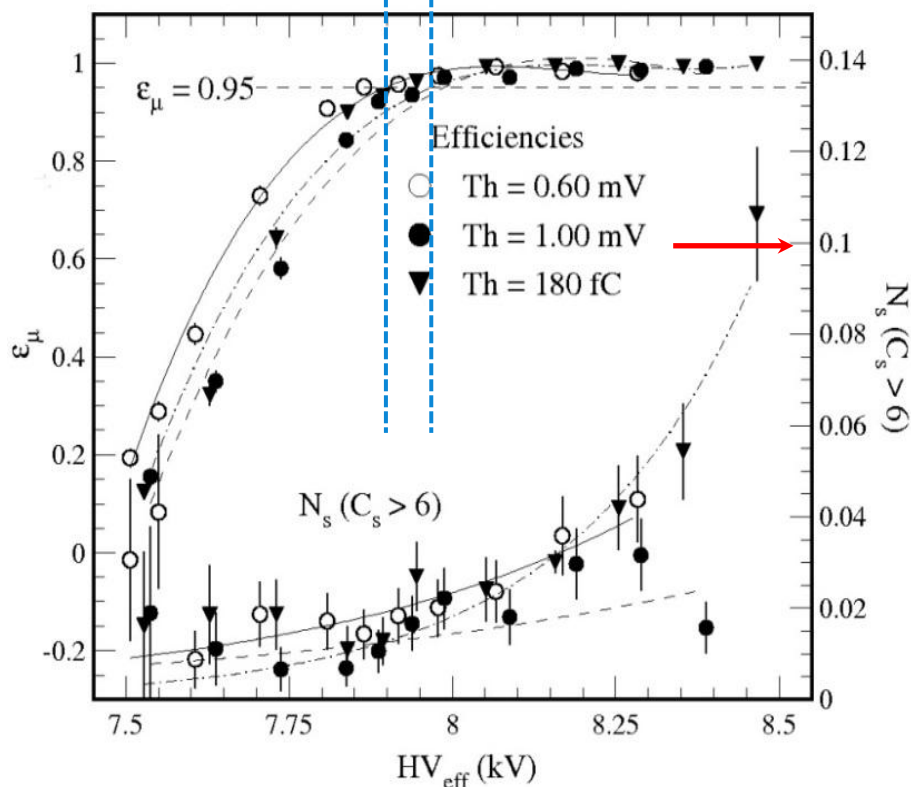
The difference in HVs yielding 95-% efficiencies at  $Th = 0.6$  mV and 1.0 mV (or  $\sim 180$  fC)  $\sim 70$  V.

But, threshold dependences of  $C_s$  and  $N_s$  are much larger.

70 V

1<sup>st</sup>  $\eta$  region (mean strip pitch  $\sim 12$  mm)

Usable range defined by  $\epsilon > 0.95$  &  $N_s(C_s > 6 < 10\%)$



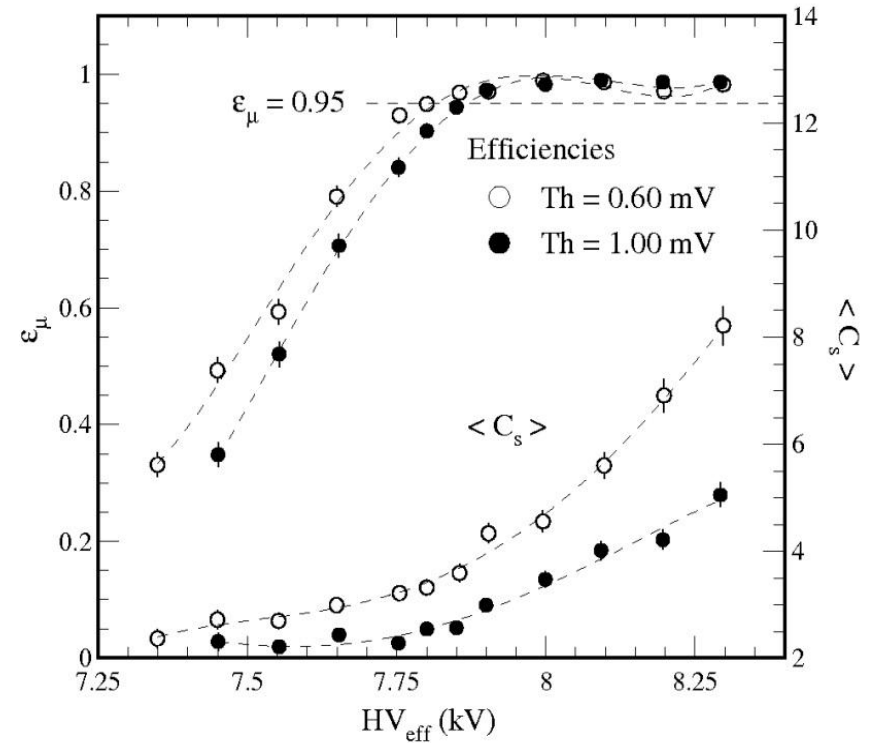
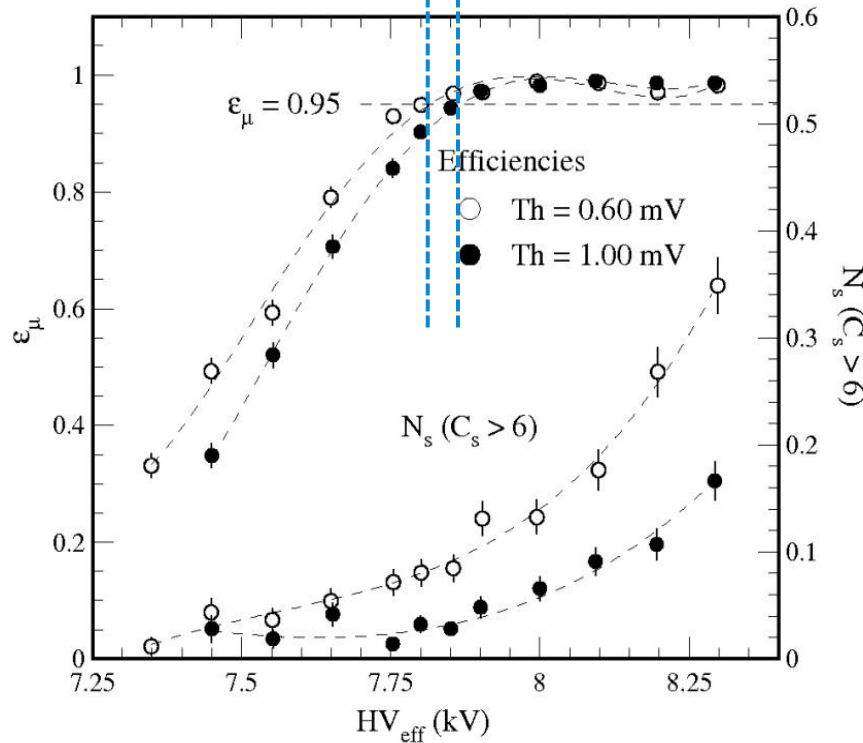
Realized that the threshold dependences of  $C_s$  and  $N_s$  are more severe for narrower strips.

→ Needs proper terminations with the matched strip impedance in FEBs.

Or, needs fine tuning of threshold values to adapt various strip pitches.

3<sup>rd</sup>  $\eta$  region (mean strip pitch  $\sim 8.5$  mm)

50 V Usable range defined by  $\epsilon > 0.95$  &  $N_s(C_s > 6 < 10\%)$





# Multi-gap (4-gap) RPC (cosmic muons at KODEL)

Gas : 95.2% TFE + 4.5%  $iC_4H_{10}$  + 0.3%  $SF_6$  + water vapor (0.3% in mass ratio)

## Less strong threshold dependence of efficiencies & mean cluster sizes

Measured the muon data only with the new FEBs.

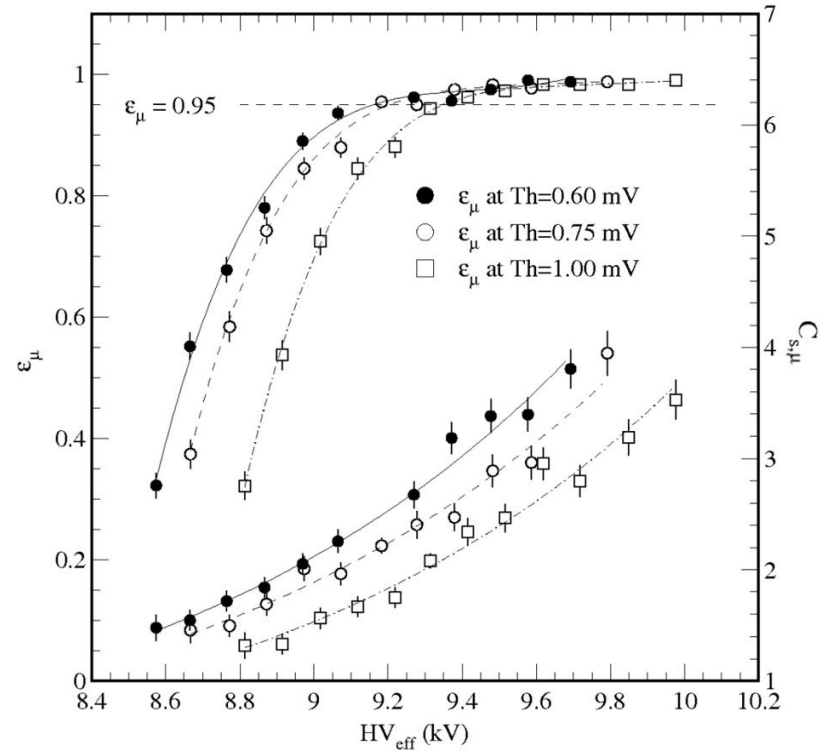
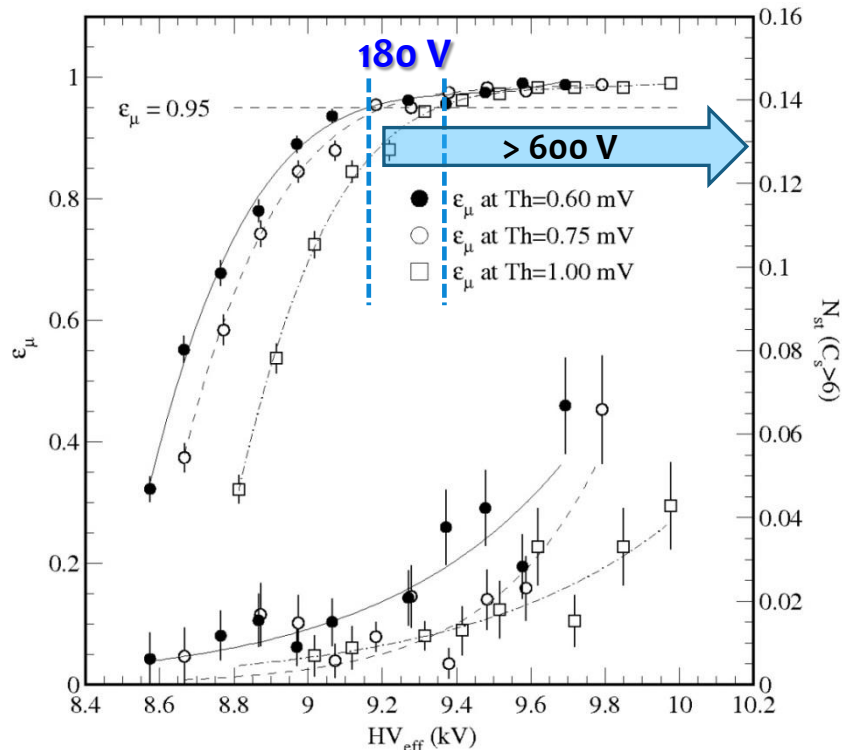
The difference in HVs yielding 95-% efficiencies measured at  $Th = 0.6$  mV and  $1.0$  mV  $\sim 200$  V.

✓ The usable size of the efficiency plateau is  $> 600$  V even for the data measured at  $0.6$  mV.

→ Better to lower the digitization threshold to lower the gain of signals.

Usable range defined by  $\epsilon_\mu > 0.95$  &  $N_s(C_s > 6 < 10\%)$

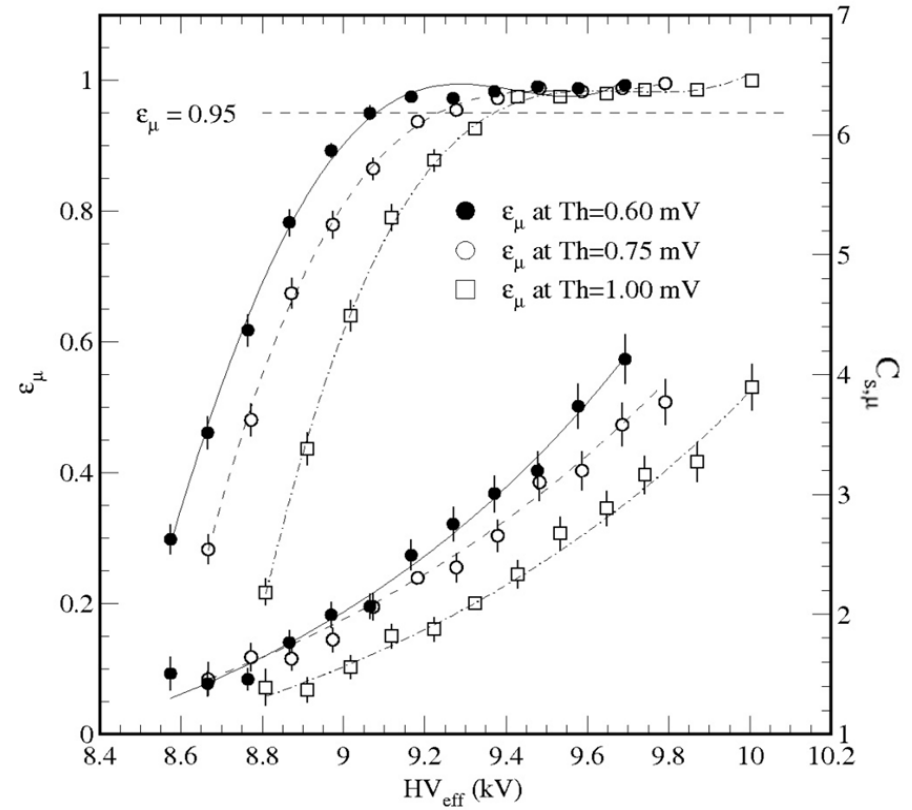
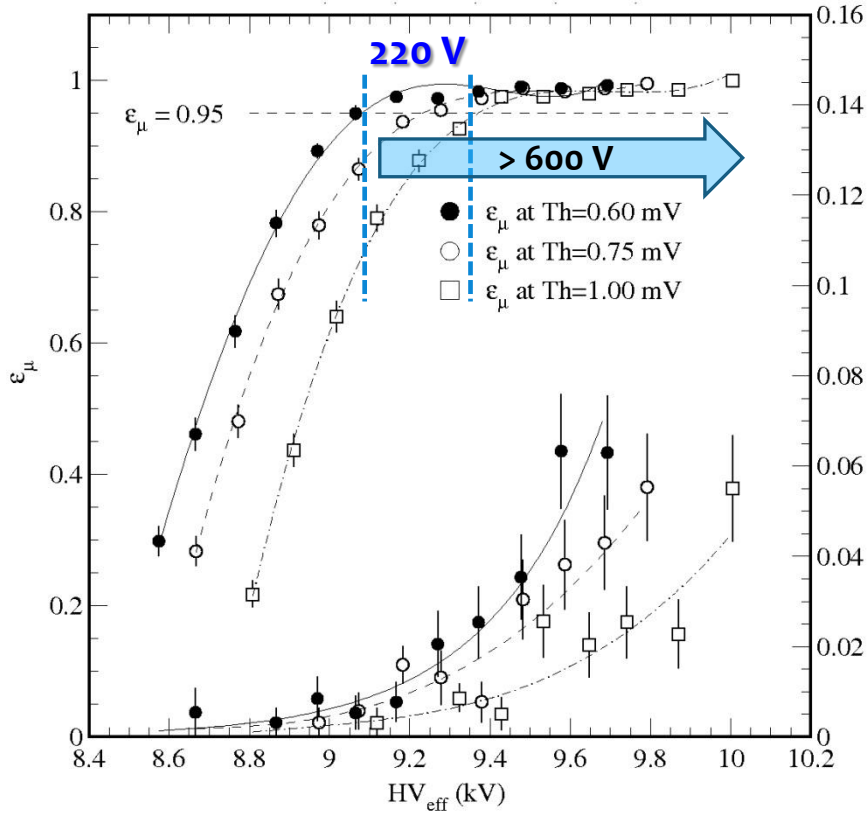
1<sup>st</sup>  $\eta$  region (mean strip pitch  $\sim 12$  mm)



# Multi-gap RPCs are less sensitive both to threshold and strip pitch

3<sup>rd</sup>  $\eta$  region (mean strip pitch  $\sim 8.5$  mm)

Usable range defined by  $\epsilon > 0.95$  &  $N_s(C_s > 6 < 10\%)$



# Double-gap and Multi-gap (4-gap) RPCs tested with H4 beams at GIF++

## Threshold dependence of efficiencies (muon beam only)

Reconstructed of strip-hit clusters and applied proper cuts:

3<sup>rd</sup>  $\eta$  region (mean strip pitch  $\sim 8.5$  mm)

**Time + Geometry + Beam area**

Double-gap RPC: Difference in HVs yielding 95%-efficiencies at Th = 170 and 240 fC  $\sim 70$  V.

Multi-gap RPC: Difference in HVs yielding 95%-efficiencies at Th = 170 and 240 fC  $\sim 140$  V.

### Thresholds for CMS RPC FEE

LV 220 mV  $\Leftrightarrow$  170 fC

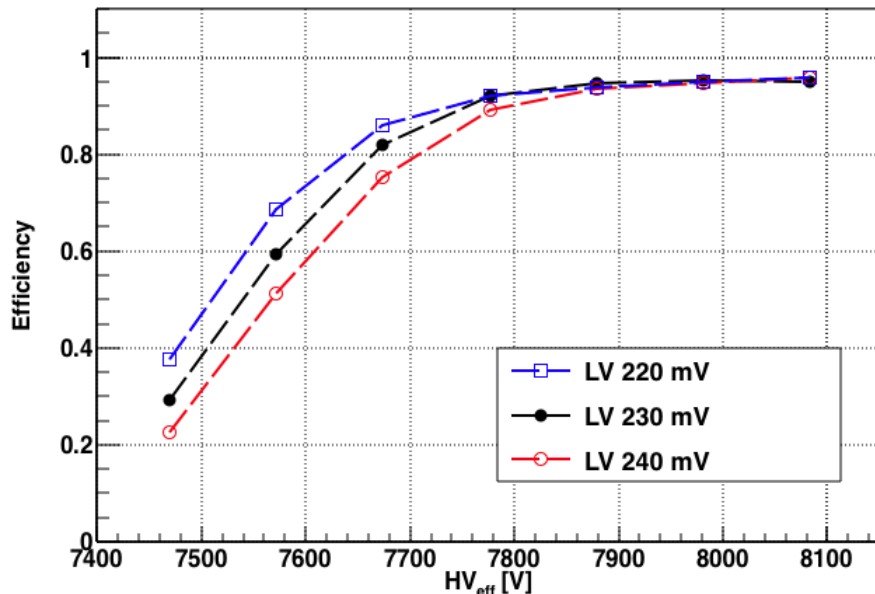
LV 230 mV  $\Leftrightarrow$  190 fC

LV 240 mV  $\Leftrightarrow$  240 fC

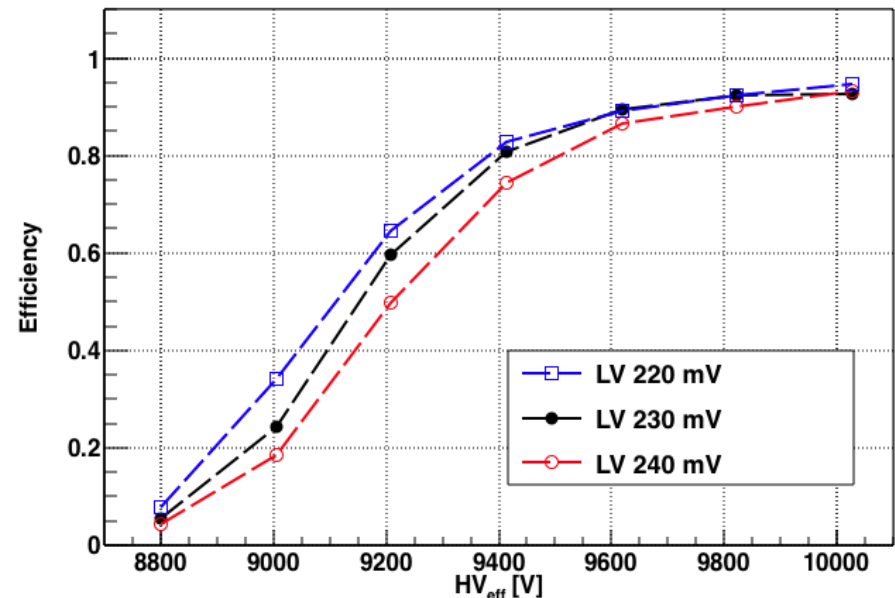
## Double-gap RPC

## Multi-gap RPC

KODEL Double-gap, Oct 2015 Test Beam, Att. 21.5



KODEL Multi-gap, Oct 2015 Test Beam, Att. 21.5



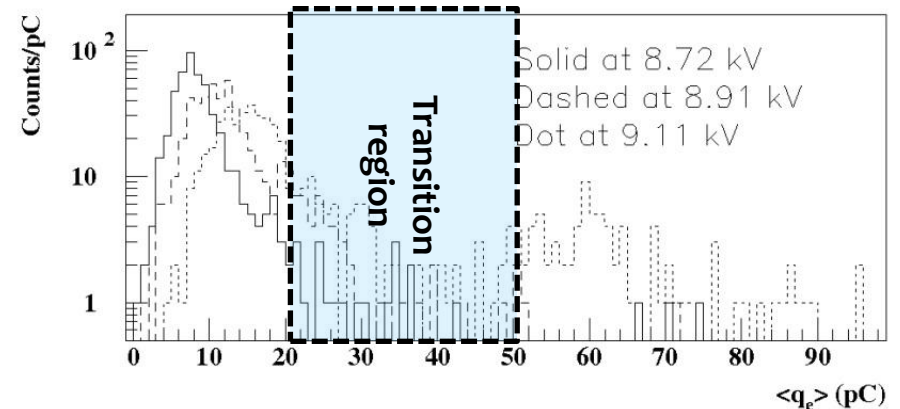
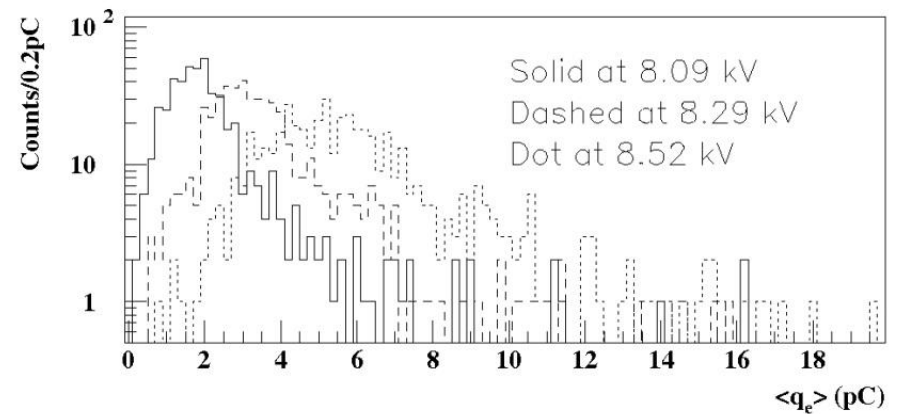
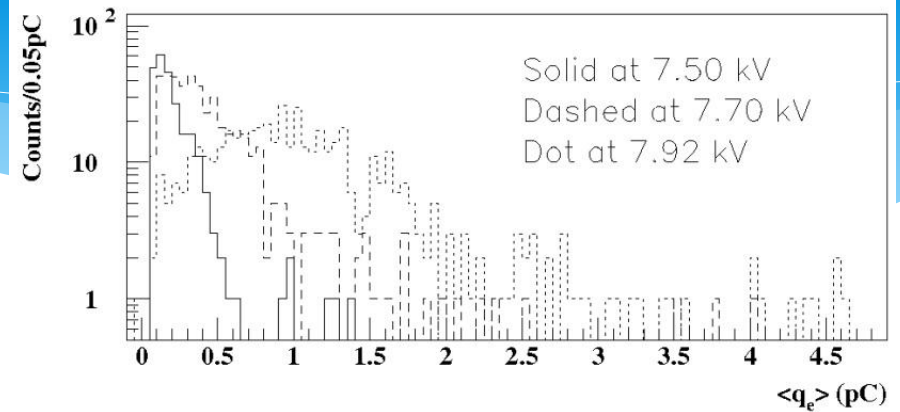
# Charge spectra (using FADCs)

## To understand the dynamic ranges of operation

- Gas = 95.1% TFE + 4.5%  $iC_4H_{10}$  + 0.4%  $SF_6$
- Strip pitch = 12.0 mm (mid of 1<sup>st</sup>  $\eta$  section)
- Maximum time to measured = 320 ns
- ADC charges calibrated using a pulse generator

## Double-RPC RPCs

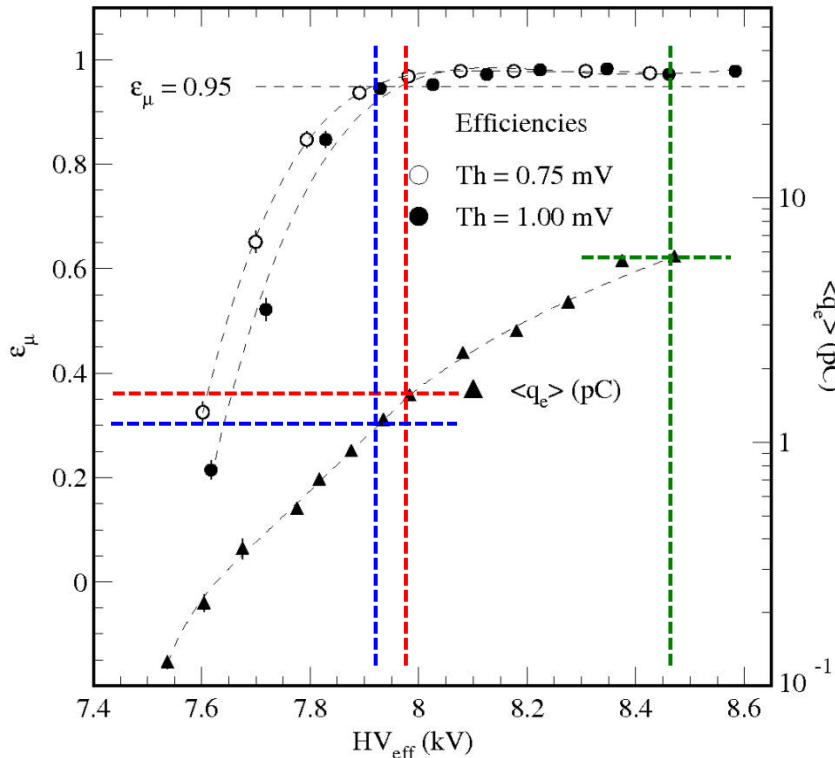
- The streamer probability  $N_s$  was defined as  $q_e > 20$  pC (in the TDC data,  $C_s > 6$ )
- Transition region between avalanche and streamer regions lying in  **$20 \text{ pC} < q_e < 50 \text{ pC}$** .



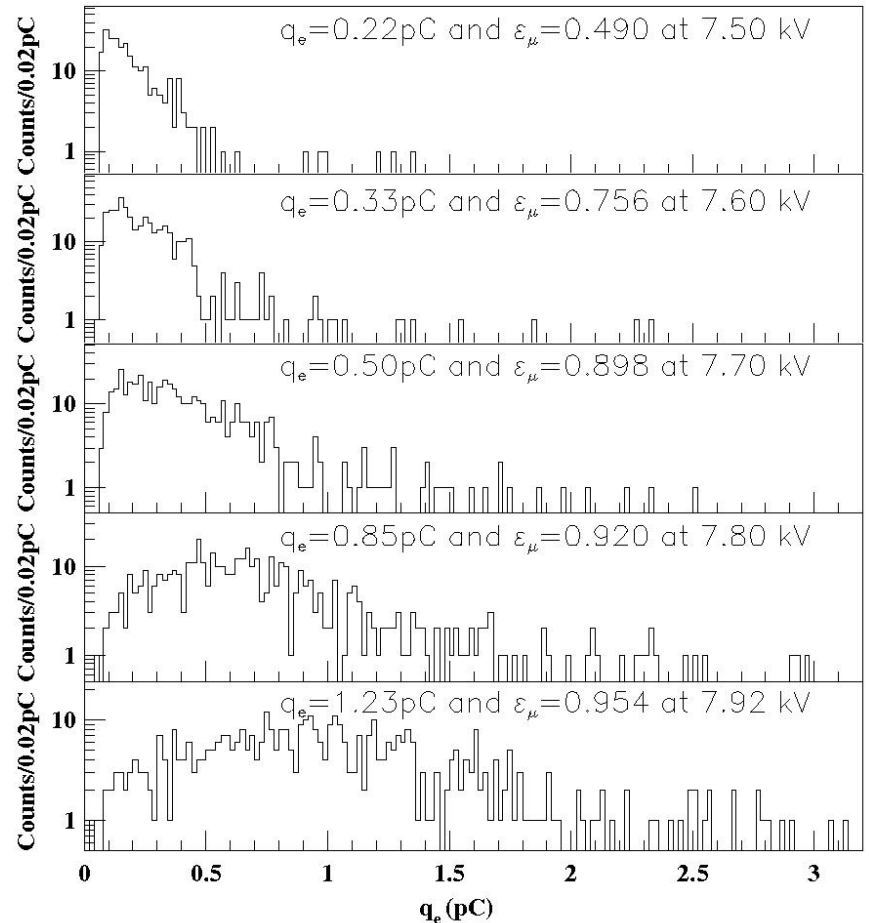


# Double-gap RPCs

- ❖ The exponential growth of the pickup charges **becomes less stiffer near  $\langle q_e \rangle \sim 1 \text{ pC}$** .  
 → Can expect that a wider usable range for the operation obtained with  $\text{Th} = 180 \text{ fC}$  (or  $1.0 \text{ mV}$ ).
- ❖ As lowering the threshold, the usable plateau range is getting narrower.  
 → Found no advantage of choosing lower thresholds.



- $\langle q_e \rangle \sim 1.65 \text{ pC}$  at  $\epsilon_\mu = 0.95$  ( $\text{Th} = 1.0 \text{ mV}$ )
- $\langle q_e \rangle \sim 1.30 \text{ pC}$  at  $\epsilon_\mu = 0.95$  ( $\text{Th} = 0.6 \text{ mV}$ )
- $\langle q_e \rangle \sim 5.5 \text{ pC}$ : limit of avalanche mode

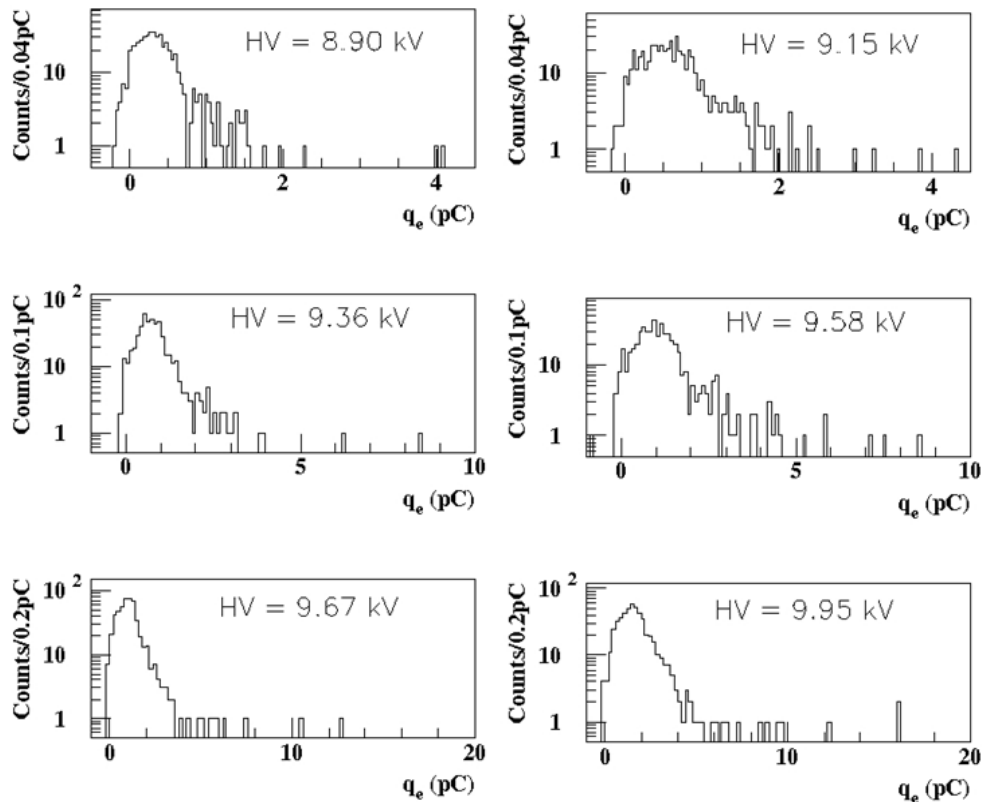


# Charge spectra (using FADCs) for Multi-gap RPCs

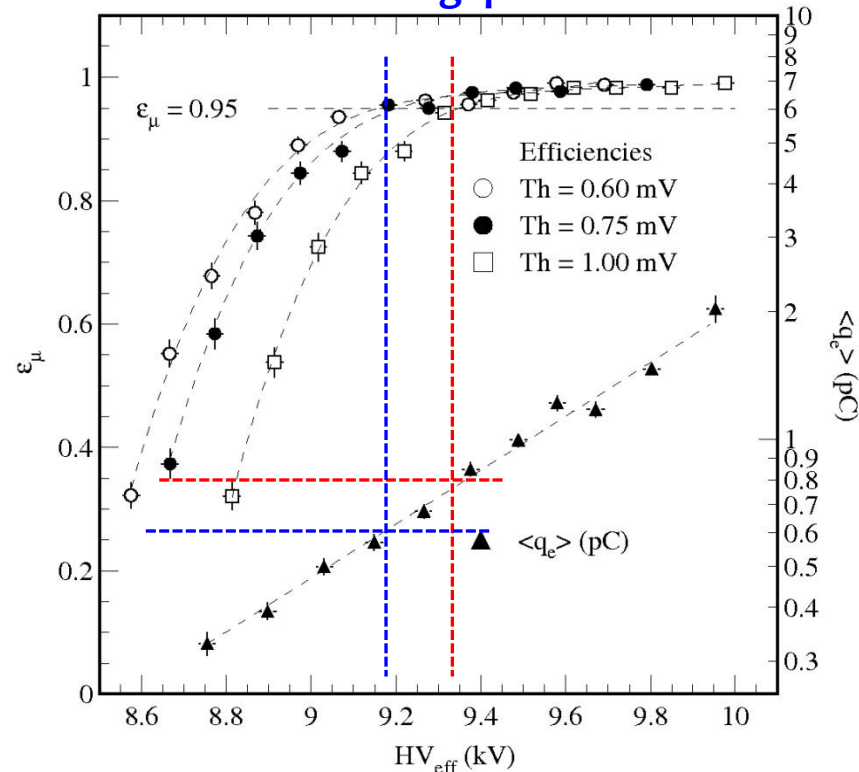
The slope of the exponential growth is saturated even **at very low  $\langle q_e \rangle$** .

This is the reason why the wide usable plateau range was obtained even with  $\text{Th} = 0.6 \text{ mV}$ .

→ Better to adopt lower thresholds to enhance the detector sensitivity to **maximize the rate capability** and while to **minimize aging** due to high-rate beam background.



## 0.8-mm four-gap RPC

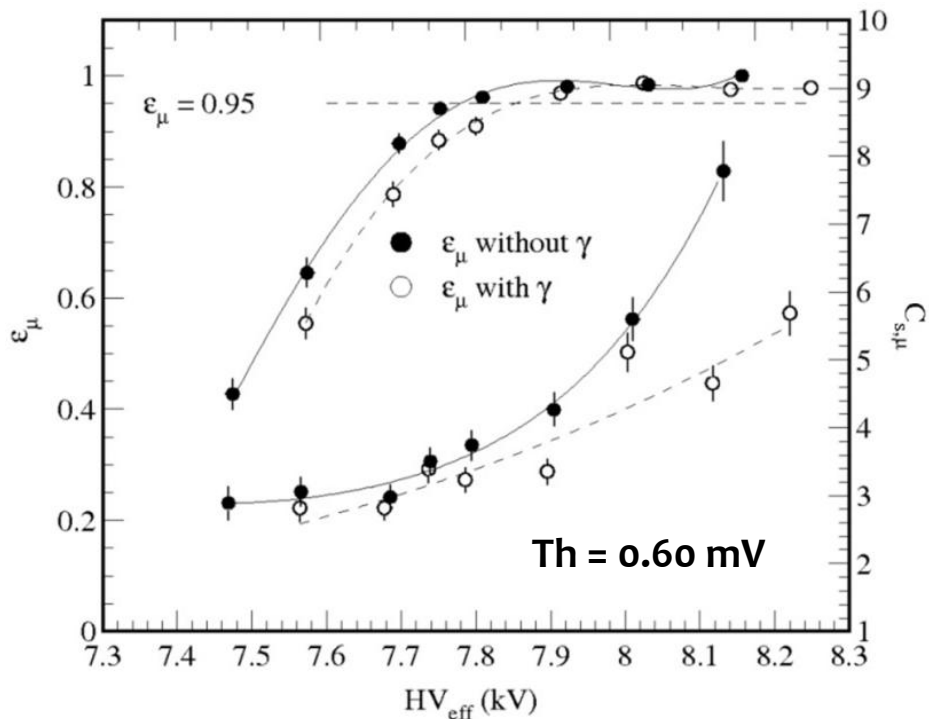


# Influence of gamma rates measured at KODEL (5.55 GBq $^{137}\text{Cs}$ )

- ✓ Tagged cosmic muons with/without presence of gamma background
- ✓ Installed each testing RPC at 37 cm from source → **Gamma flux =  $0.32\text{ MHz cm}^{-2}$**   
**Irradiation area ~  $1000\text{ cm}^{-2}$  → max.  $\gamma$  rates in 2-gap or 4-gap RPCs ~  $1.4\text{ kHz cm}^{-2}$**

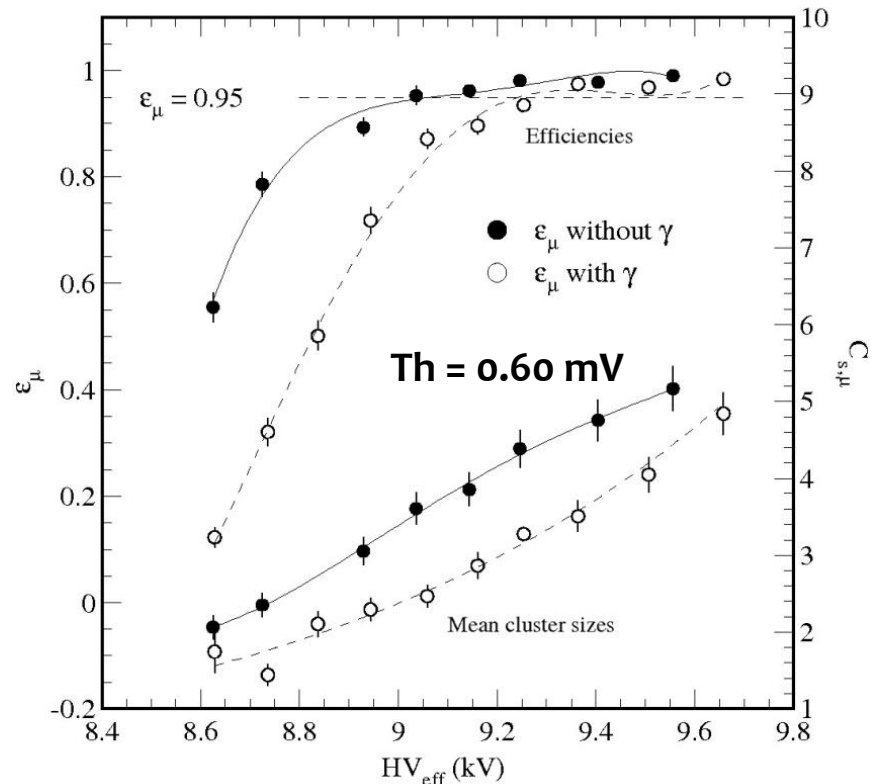
## Double-gap RPC

Shift @  $\epsilon=0.95$  in HV due to the  $\gamma$  background  **$\sim 70\text{ V}$**   
 (yielding  $\sim 1\text{ kHz cm}^{-2}$  at the mid of the plateau)  
 → **Rate capability  $\gg 1\text{ kHz cm}^{-2}$**



## Multi-gap RPC

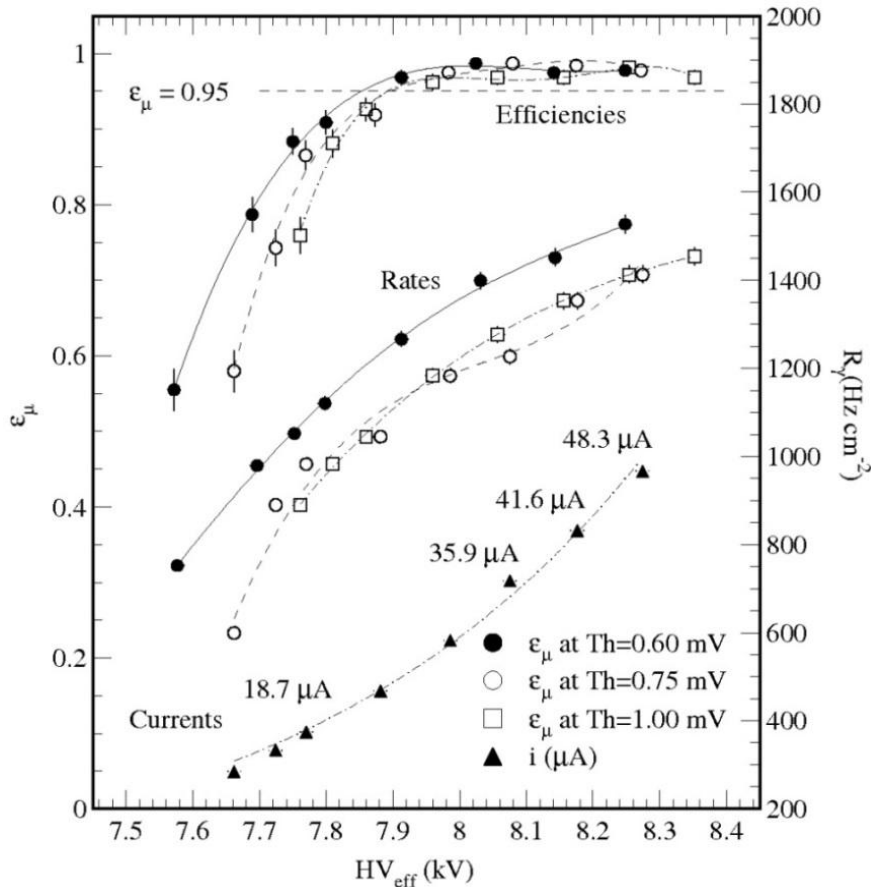
Shift @  $\epsilon=0.95$  in HV due to  $\gamma$   **$\sim 200\text{ V}$**   
 (larger than the 2-gap RPC case)  
**But, confirmed the rate capability  $\sim 5\text{ kHz cm}^{-2}$**



# $\gamma$ rates and currents (KODEL)

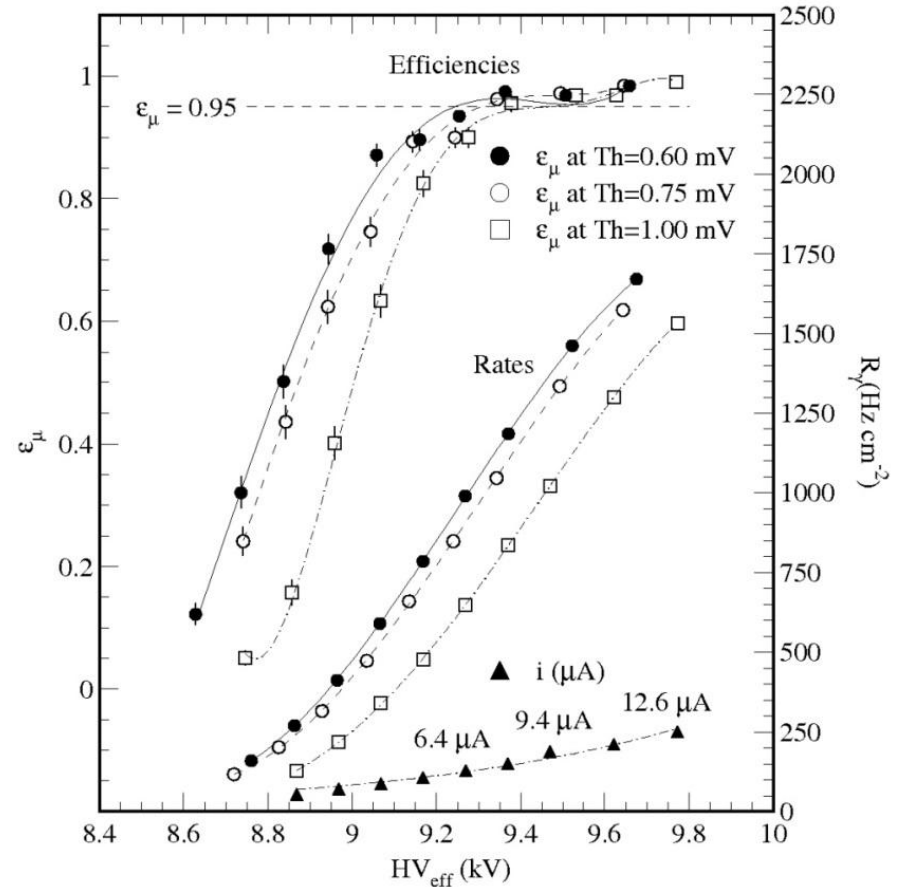
## Double-gap RPC

- ✓ Detector efficiency for 662-keV  $\gamma \sim 60\%$  of Q.E. (by GEANT) at  $HV_{\epsilon=0.95} + 150 \text{ V}$ .
- ✓  $\langle Q_{e,\gamma} \rangle \sim 25 \text{ pC}$  at  $HV_{\epsilon=0.95} + 150 \text{ V}$ .



## Multi-gap RPC

- ✓ Detector efficiency for 662-keV  $\gamma \sim 40\%$  of Q. E. (by GEANT) at  $HV_{\epsilon=0.95} + 200 \text{ V}$ .
- ✓  $\langle Q_{e,\gamma} \rangle \sim 6.5 \text{ pC}$  at  $HV_{\epsilon=0.95} + 200 \text{ V}$ .
- **$\sim 4$  times smaller than the 2-gap RPC case**





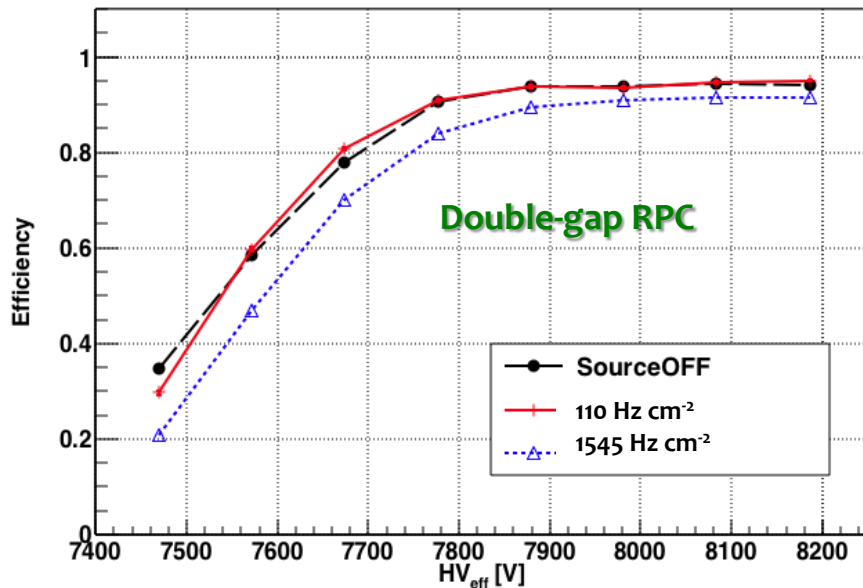
# Rate dependence of efficiencies measured at GIF++ (1.4 TBq $^{137}\text{Cs}$ )

Shift @  $\epsilon=0.95$  in HV due to  $\gamma$  background  $\sim 70\text{ V}$  for the double-gap RPC

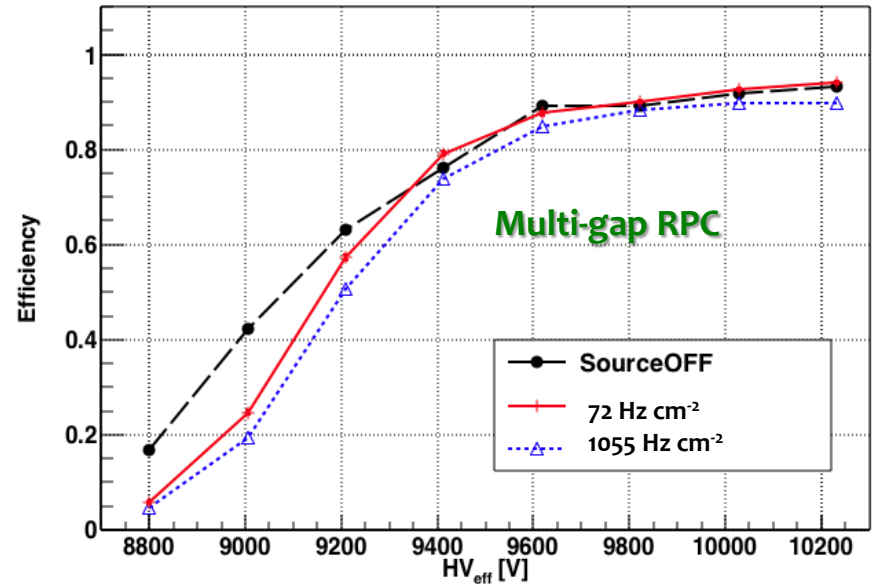
Shift @  $\epsilon=0.95$  in HV due to  $\gamma$  background  $\sim 100\text{ V}$  for the multi-gap RPC

## Efficiencies (just subtracted for gamma background)

KODEL Double-gap, GIF++ Oct 2015 Test Beam, LV-230mV



KODEL Multi-gap, GIF++ Oct 2015 Test Beam, LV-230mV



# Double-gap RPCs: Long tails in $C_s$ distributions (KODEL and GIF++)

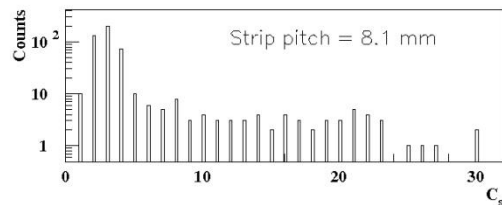
- ✓ Stronger capacitive coupling due to **no strip termination and impedance mismatching**.
- ✓ The trend is more severe when measured at the low threshold and with narrower-pitch strips  
→ Needs proper terminations with the matched strip impedance in FEBs.

Fixed input impedance at CMS-RPC FEBs = 15  $\Omega$

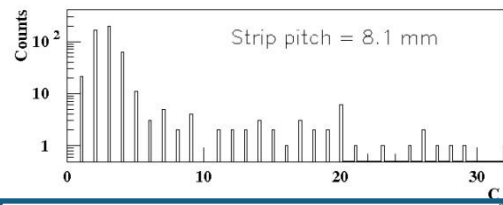
**Th = 0.6 mV**   **KODEL**   **No source**   **Th = 1.0 mV**

**GIF++**

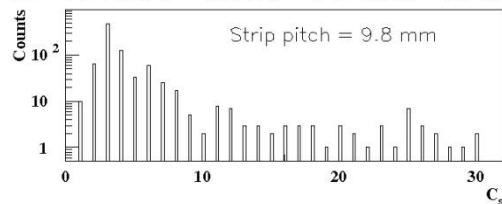
HV = 8.00 kV,  $C_s = 4.56$ ,  $N_s = 0.1327$ , Th = 0.6 mV



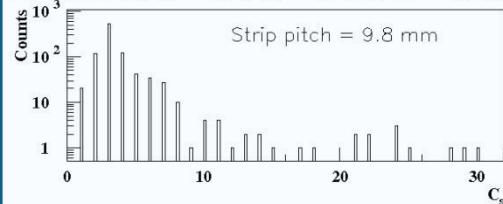
HV = 8.09 kV,  $C_s = 4.01$ ,  $N_s = 0.0909$ , Th = 1.0 mV



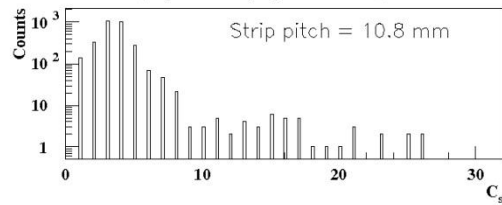
HV = 7.98 kV,  $C_s = 4.89$ ,  $N_s = 0.1246$ , Th = 0.6 mV



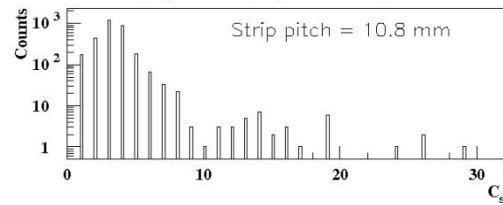
HV = 8.08 kV,  $C_s = 4.11$ ,  $N_s = 0.0728$ , Th = 1.0 mV



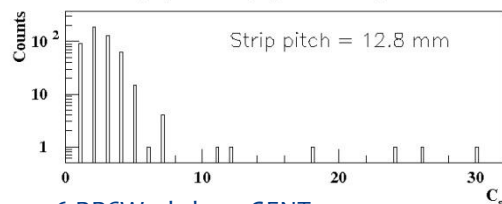
HV = 7.98 kV,  $C_s = 3.93$ ,  $N_s = 0.0385$ , Th = 0.6 mV



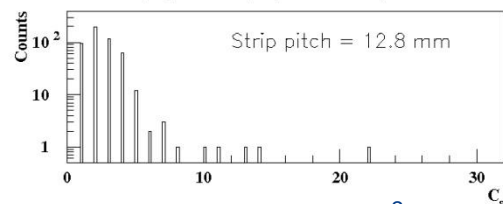
HV = 8.08 kV,  $C_s = 3.71$ ,  $N_s = 0.0330$ , Th = 1.0 mV



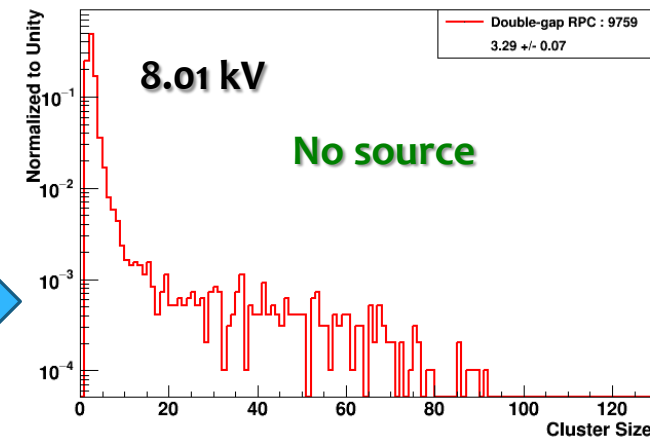
HV = 7.98 kV,  $C_s = 2.93$ ,  $N_s = 0.0201$ , Th = 0.6 mV



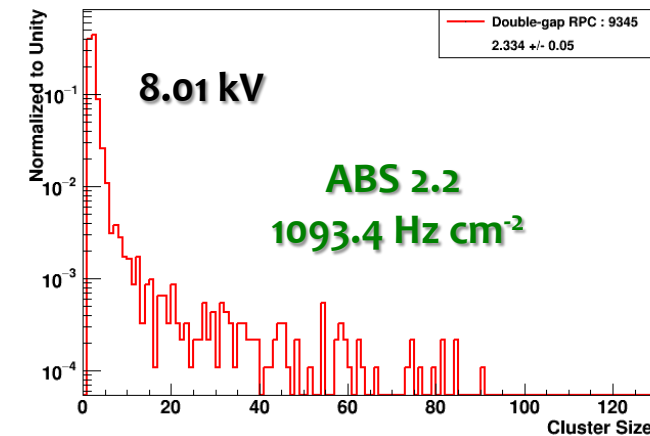
HV = 8.09 kV,  $C_s = 2.55$ ,  $N_s = 0.0181$ , Th = 1.0 mV



KODEL Double-gap, GIF++ Oct 2015 Test Beam, Source OFF, LV-230mV, HV-7700V



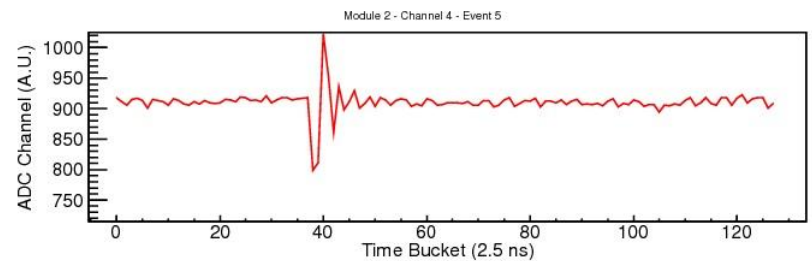
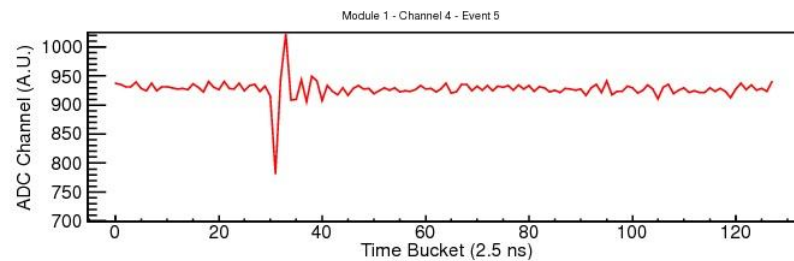
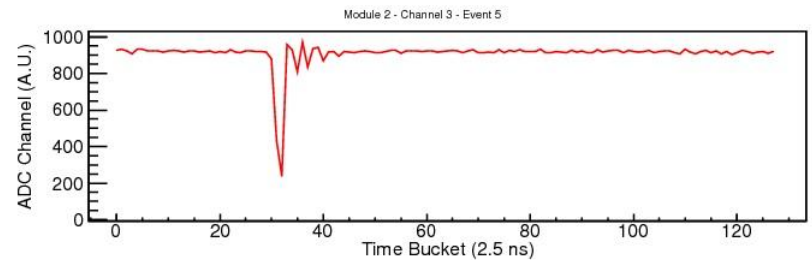
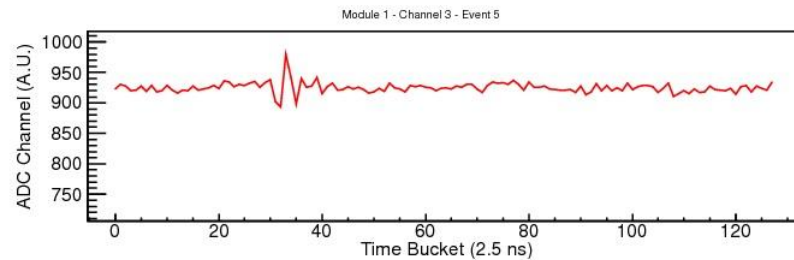
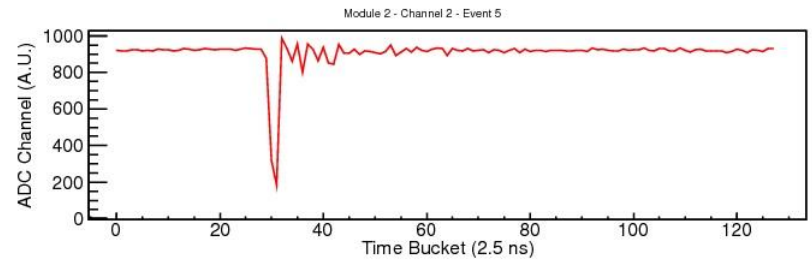
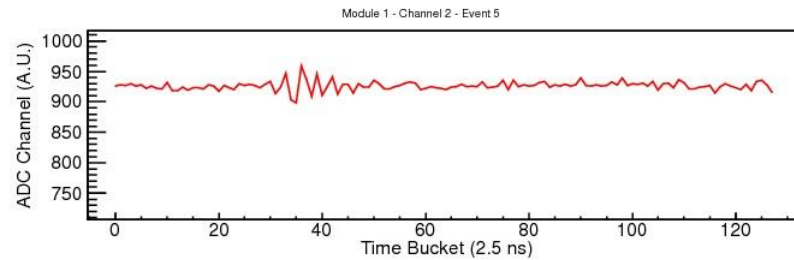
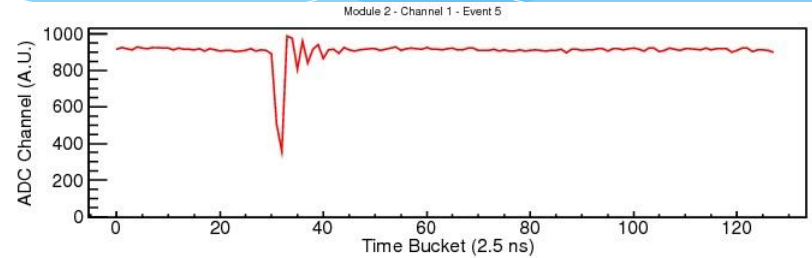
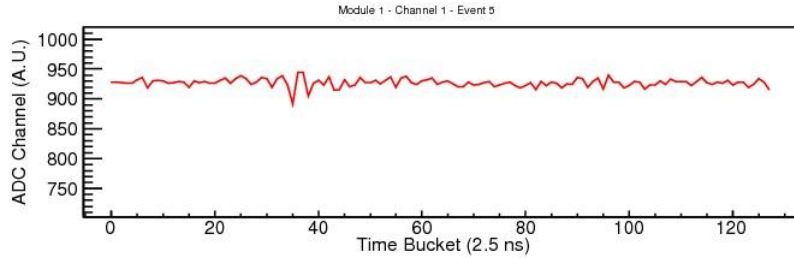
KODEL Double-gap, GIF++ Oct 2015 Test Beam, Att. 2.2, LV-230mV, HV-7700V



# Strong capacitive couplings among narrow-pitch strips (measured FADCs)

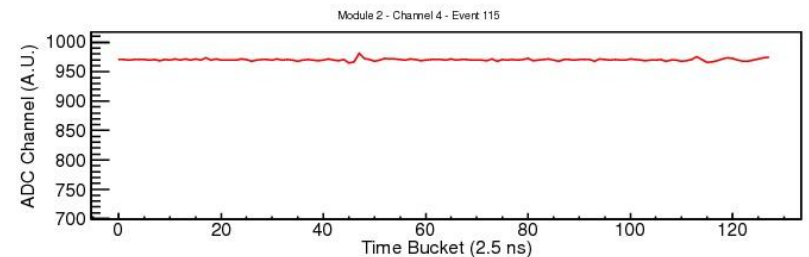
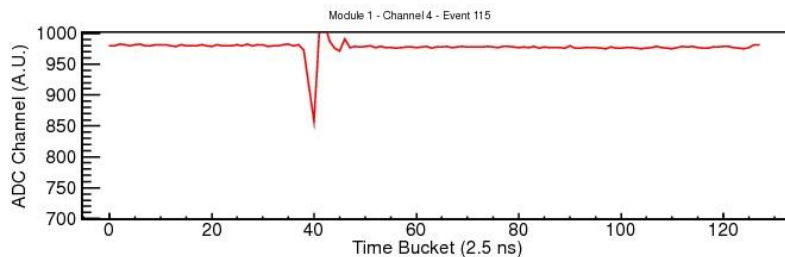
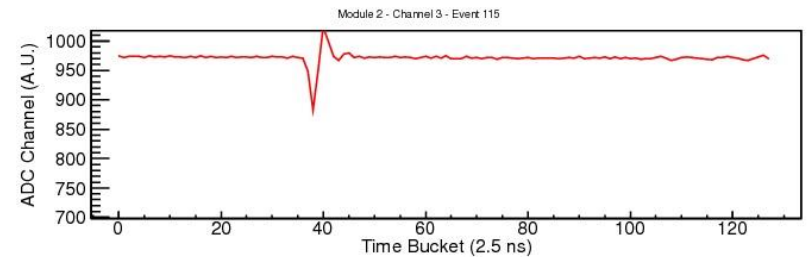
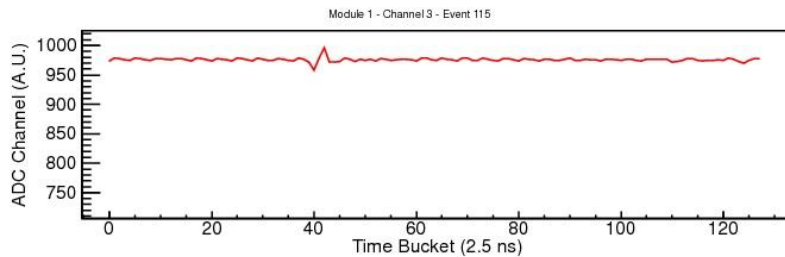
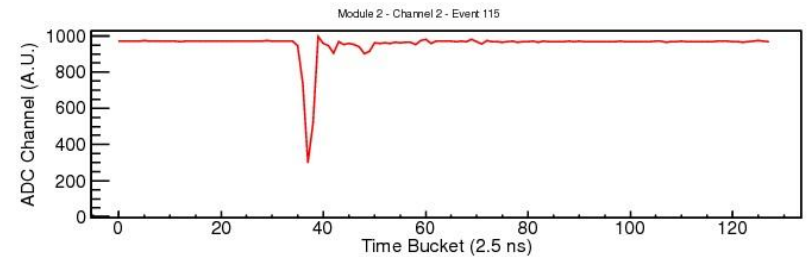
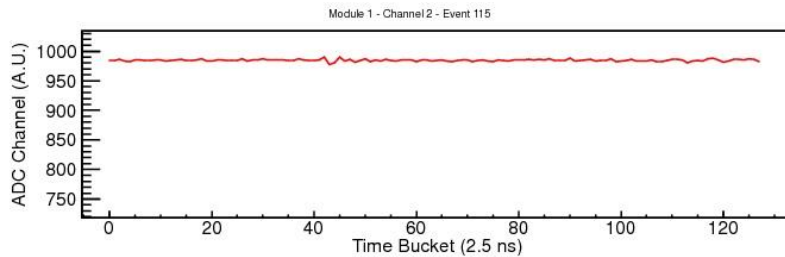
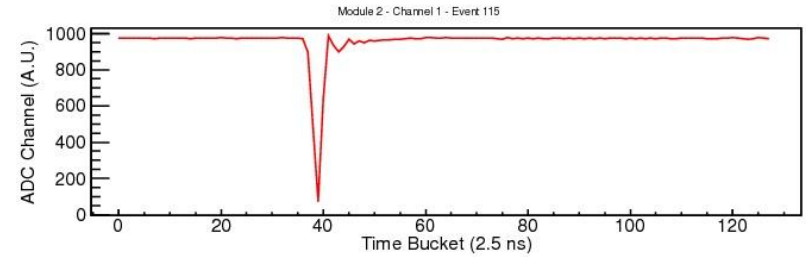
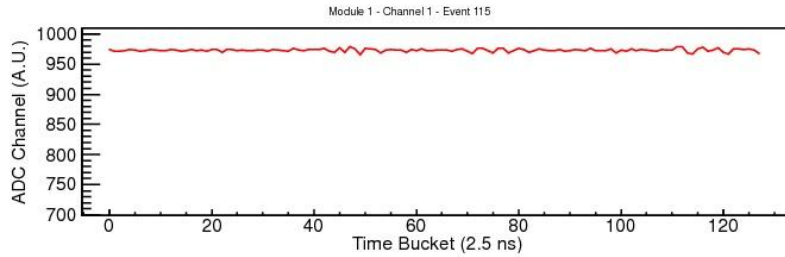
Muon pulses tagged at a region with strip pitch of  $\sim 11.0$  mm

Cross talks  $\sim 15\%$



# Muon signals of the same detector but with strip pitches of $\sim 22.0$ mm

Capacitive couplings are less severe with wider-pitched strips.





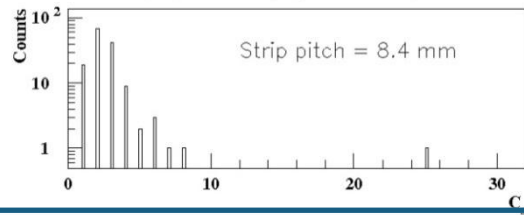
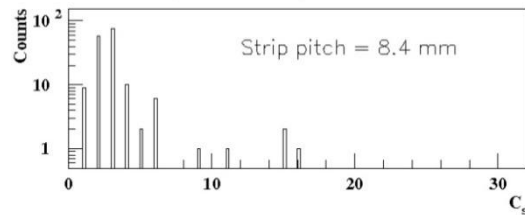
# Multi-gap RPC: Tails in cluster-size distributions (KODEL & GIF++)

- ✓ The tails are less severe for multi-gap RPCs
- ✓ The threshold and pitch dependences are also lower.

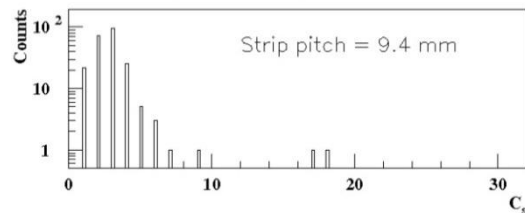
**Th = 0.6 mV** **KODEL** **No source** **Th = 1.0 mV**

**GIF++** Fixed input impedance at CMS-RPC FEBs = 15 Ω

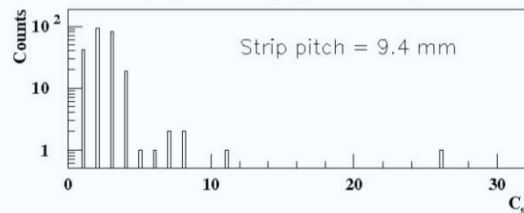
HV = 9.37 kV,  $C_s = 3.141$ ,  $N_s = 0.0301$ , Th = 0.6 mV    HV = 9.53 kV,  $C_s = 3.086$ ,  $N_s = 0.0274$ , Th = 1.0 mV



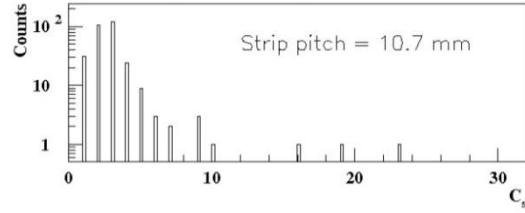
HV = 9.37 kV,  $C_s = 3.647$ ,  $N_s = 0.0460$ , Th = 0.6 mV



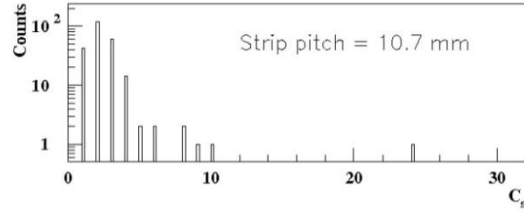
HV = 9.53 kV,  $C_s = 2.828$ ,  $N_s = 0.0246$ , Th = 1.0 mV



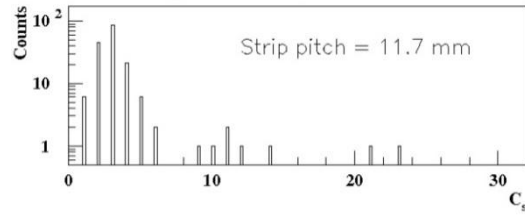
HV = 9.37 kV,  $C_s = 3.142$ ,  $N_s = 0.0361$ , Th = 0.6 mV



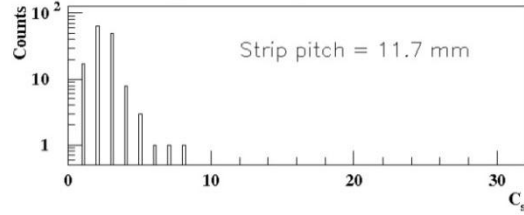
HV = 9.52 kV,  $C_s = 2.695$ ,  $N_s = 0.0205$ , Th = 1.0 mV



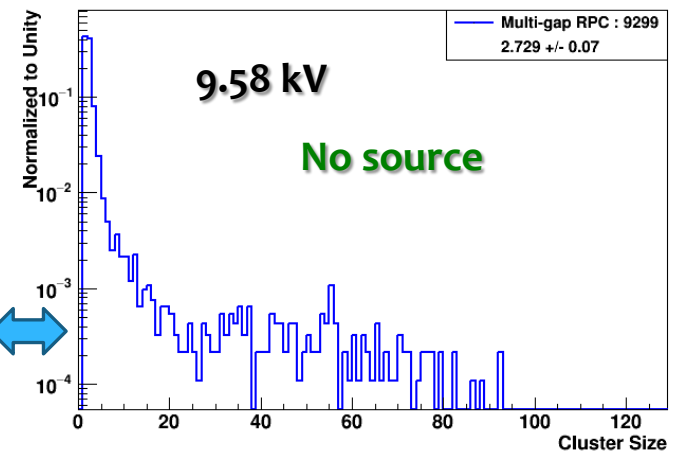
HV = 9.37 kV,  $C_s = 3.232$ ,  $N_s = 0.0220$ , Th = 0.6 mV



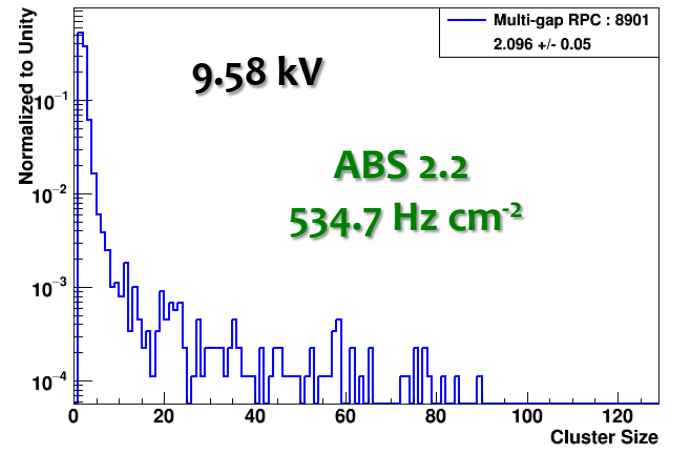
HV = 9.52 kV,  $C_s = 2.550$ ,  $N_s = 0.0139$ , Th = 1.0 mV



KODEL Multi-gap, GIF++ Oct 2015 Test Beam, Source OFF, LV-230mV, HV-9400V



KODEL Multi-gap, GIF++ Oct 2015 Test Beam, Att. 2.2, LV-230mV, HV-9400V



## 3. Conclusions

### Confirmed the detector performances for the two different type RPCs.

#### For 1.6-mm double-gap RPCs instead of 2.0-mm gaps

1. The operational **HV = 7.8 ~ 8.4 kV** with  $T_h = 180$  fC.  
→ ~ 15% lower than the current CMS RPCs
2. The higher threshold was preferred to suppress the large  $C_s$  measured at narrower-pitch strips.  
→ **But, needs proper impedance-matched terminations, and (could be) optimization of geometrical factors (thicknesses of gaps and electrodes).**
3. Rate capability issues: shift ~ **50 V / (kHz cm<sup>-2</sup>)** in HV.  
→ **Confirmed the rate capability >> 1 kHz cm<sup>-2</sup>.**

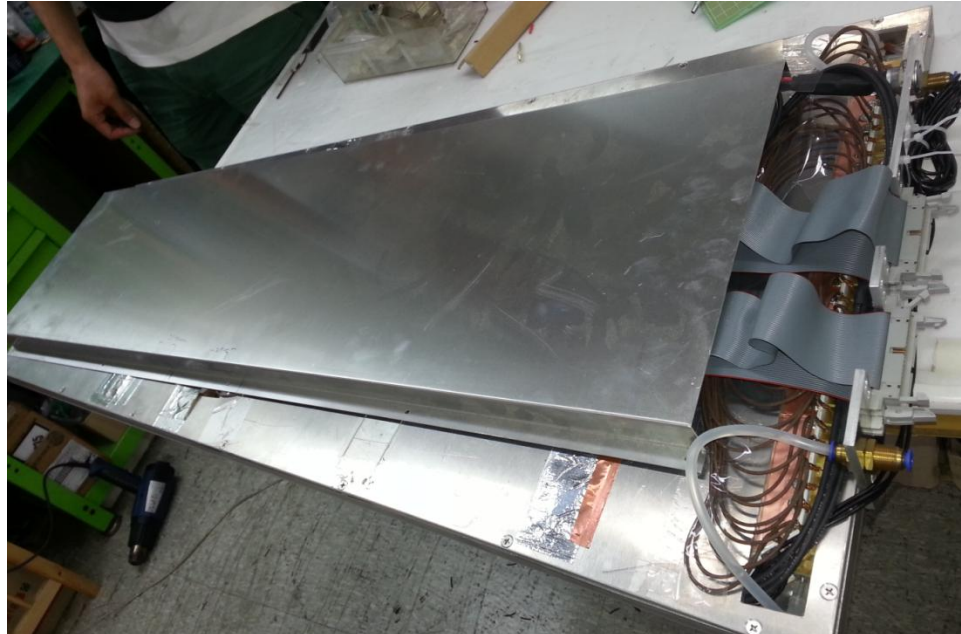
#### For 0.8-mm multi-gap(4-gap) RPCs

1. The operational **HV = 9.0 ~ 9.8 kV**
2. Lowering the threshold is more relevant compared to the 2-gap RPC case.
3. Rate capability issues:
  - ✓ Shift ~ **150 V / (kHz cm<sup>-2</sup>)** is larger than of the 2-gap RPC case **because of the floating electrodes.**
  - ✓ But, rate capability ~ **5 kHz cm<sup>-2</sup>** already confirmed in the previous R&D.
  - ✓ Gamma induced current in the 4-gap RPC ~ factor 4 smaller than the double-gap RPC case.  
→ **Better for aging.**

**In the final conclusion, both types are good candidates !**

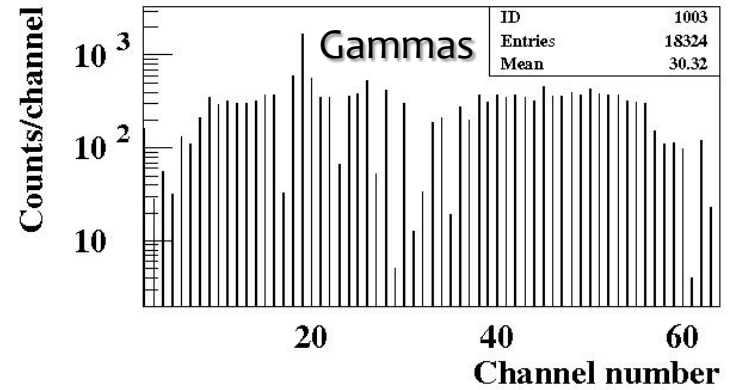
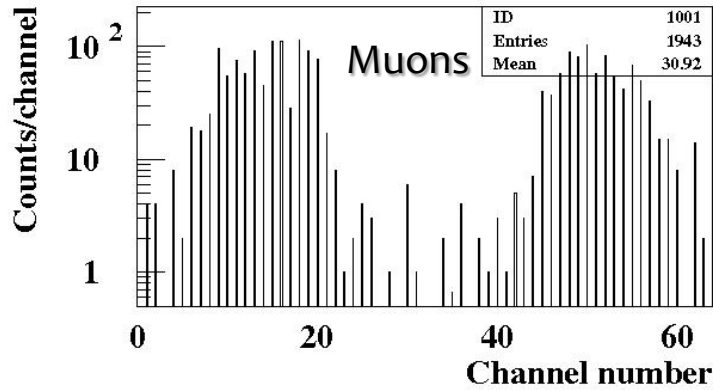


# Backups

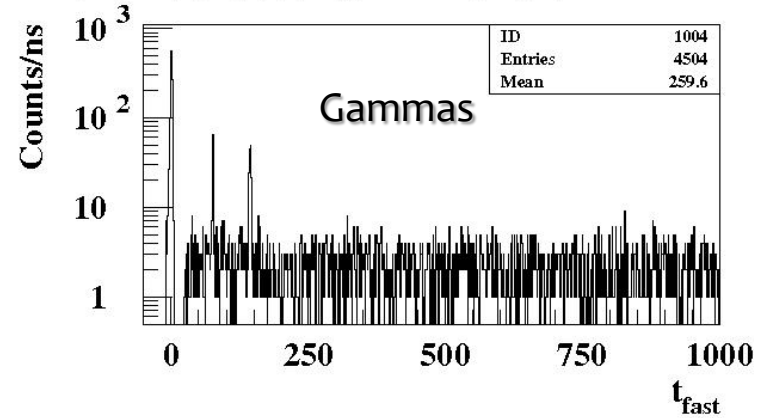
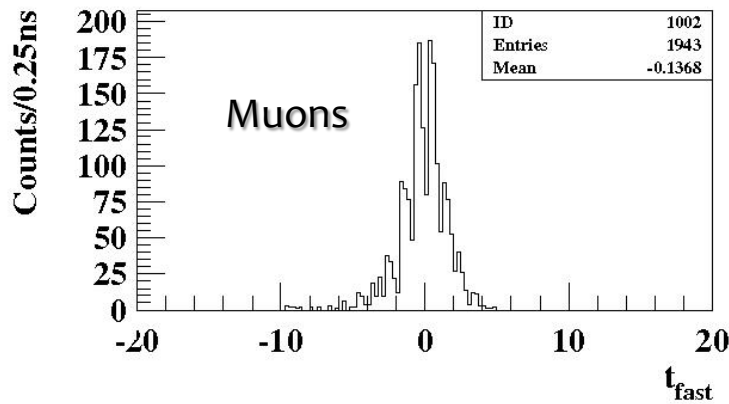


# Double-gap RPC

Muon and  $\gamma$  position distribution,  $\varepsilon = 0.9715$  at  $HV_{\text{eff}} = 7.873$  kV



Muon and  $\gamma$  time distribution,  $\varepsilon = 0.9715$  at  $HV_{\text{eff}} = 7.873$  kV





**Gamma flux = 0.32 MHz cm<sup>-2</sup> at 37 cm from  
the <sup>137</sup>Cs source measured at KODEL**

**1.6-mm double-gap RPC**

| Threshold | $\gamma$ rates (Hz cm <sup>-2</sup> )<br>(mid of plateau) | Current ( $\mu$ A)<br>(Irradiated area<br>=1000 cm <sup>2</sup> ) |
|-----------|---|---|
| 0.60 mV   | 1398.8  | 33.01   |
| 0.75 mV   | 1319.0  | 35.02   |
| 1.00 mV   | 1277.0  | 39.11   |

**0.8-mm multi-gap RPC**

| Threshold | $\gamma$ rates (Hz cm <sup>-2</sup> )<br>(mid of plateau) | Current ( $\mu$ A)<br>(Irradiated area<br>=1000 cm <sup>2</sup> ) |
|-----------|---|---|
| 0.60 mV   | 1462.1  | 8.06  |
| 0.75 mV   | 1334.9  | 9.15  |
| 1.00 mV   | 1299.0  | 9.42  |

## Strip pitch ~ 8.0 mm ( $\eta$ -section 3)

Measured at 0.6 mV (double-gap RPC)

| $HV_{\text{eff}}$ | $\epsilon$ | $\langle C_s \rangle$ | $C_s=1,2,3$ | $C_s=4,5,6$ | $C_s > 6$ |
|-------------------|------------|-----------------------|-------------|-------------|-----------|
| 7.67 kV           | 0.976      | 3.45                  | 0.796       | 0.102       | 0.082     |
| 7.77 kV           | 0.980      | 3.86                  | 0.771       | 0.139       | 0.090     |
| 7.87 kV           | 0.988      | 6.79                  | 0.494       | 0.243       | 0.289     |
| 7.97 kV           | 0.988      | 8.40                  | 0.324       | 0.300       | 0.377     |

Measured at 180 fC (Double-gap RPC)

| $HV_{\text{eff}}$ | $\epsilon$ | $\langle C_s \rangle$ | $C_s=1,2,3$ | $C_s=4,5,6$ | $C_s > 6$ |
|-------------------|------------|-----------------------|-------------|-------------|-----------|
| 7.92 kV           | 0.966      | 3.09                  | 0.810       | 0.155       | 0.035     |
| 8.02 kV           | 0.985      | 3.68                  | 0.790       | 0.190       | 0.030     |
| 8.13 kV           | 0.985      | 3.89                  | 0.654       | 0.276       | 0.047     |
| 8.21 kV           | 0.996      | 4.58                  | 0.580       | 0.369       | 0.055     |

The suppression of  $C_s$  due to the gamma background is stronger for the double-gap RPC.

## Double-gap RPC

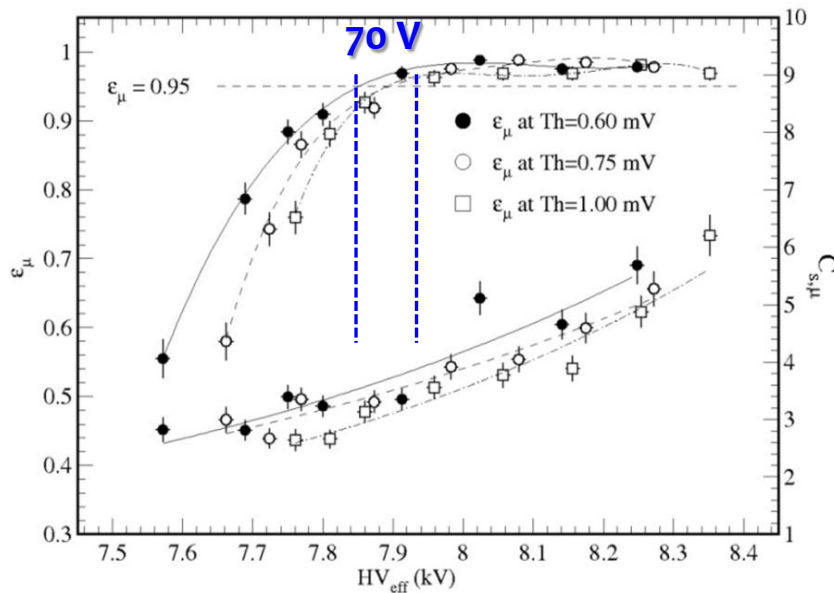
Shift @  $\epsilon=0.95$  in HV due to raising the threshold from 0.6 to 1.0 mV **~ 70 V**.

## Multi-gap RPC

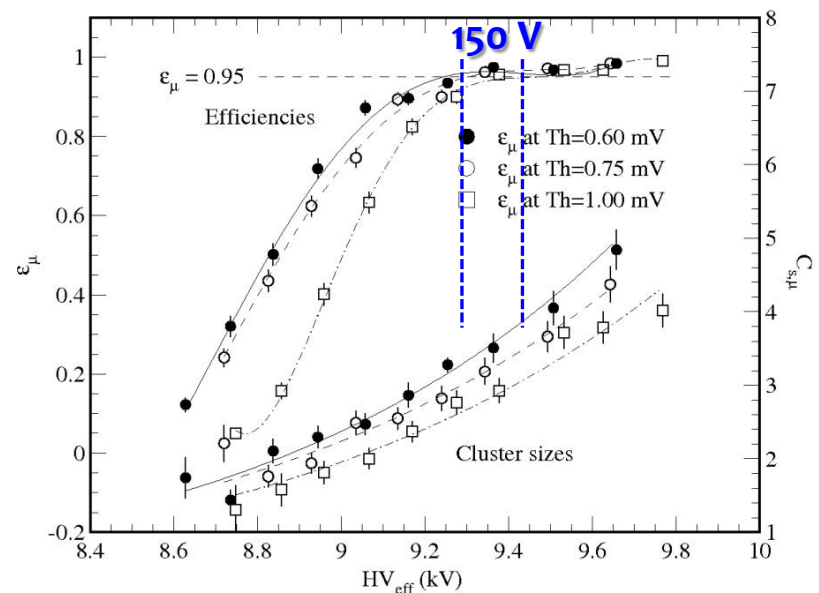
Shift @  $\epsilon=0.95$  in HV due to raising the threshold from 0.6 to 1.0 mV **~ 150 V**.

Threshold dependence **with presence of gamma background**

Double-gap RPC



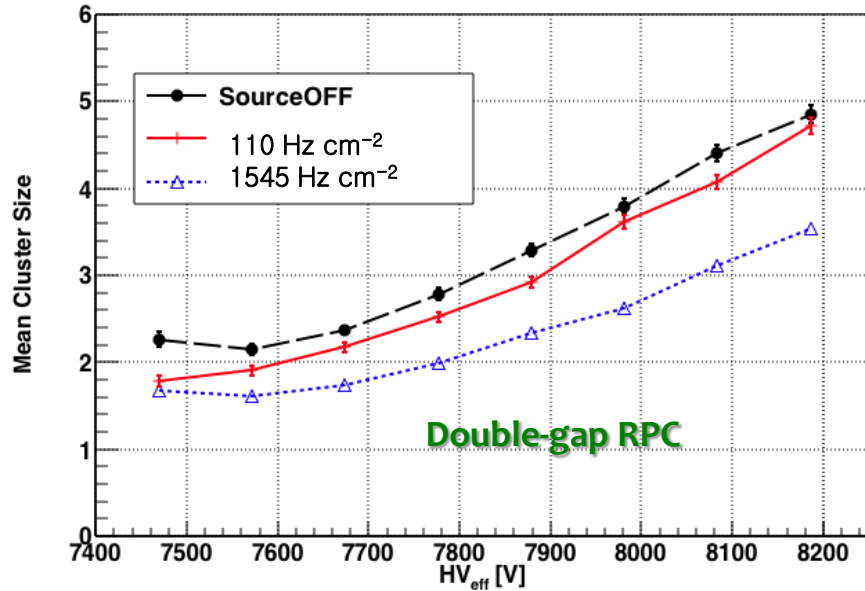
Multi-gap RPC



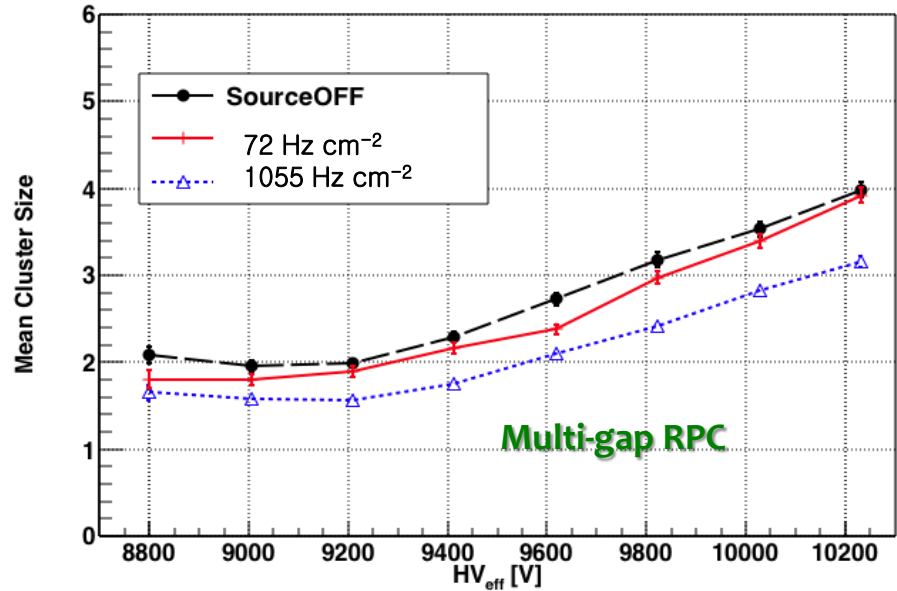
The suppression of  $C_s$  due to the gamma background is stronger for the double-gap RPC.

## Cluster sizes

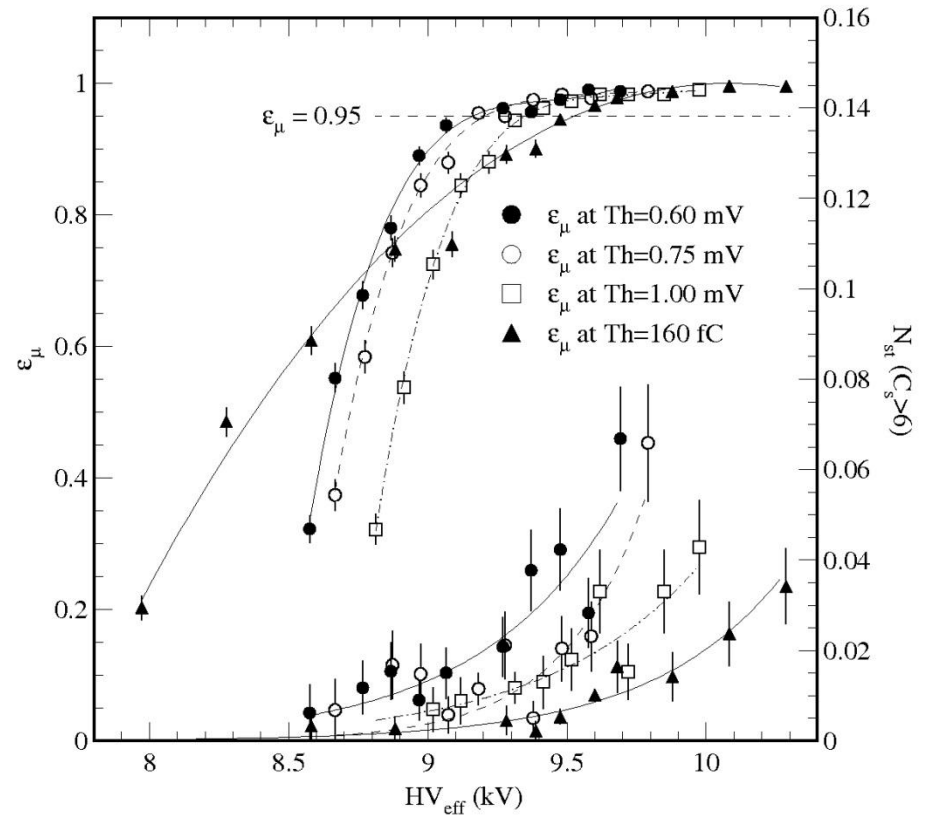
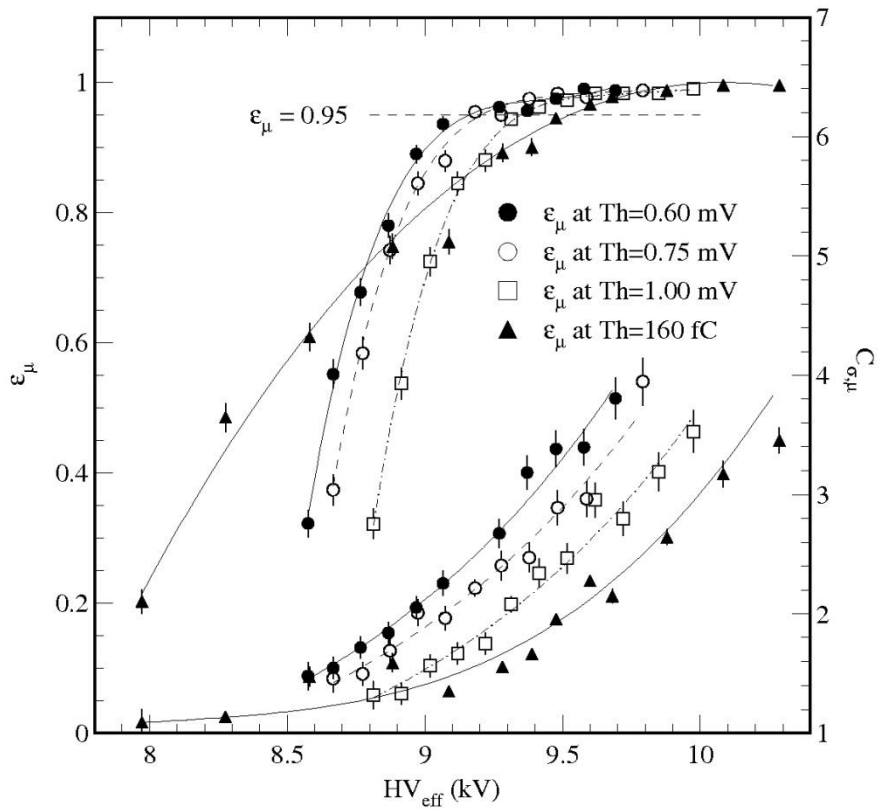
KODEL Double-gap, GIF++ Oct 2015 Test Beam, LV-230mV



KODEL Multi-gap, GIF++ Oct 2015 Test Beam, LV-230mV

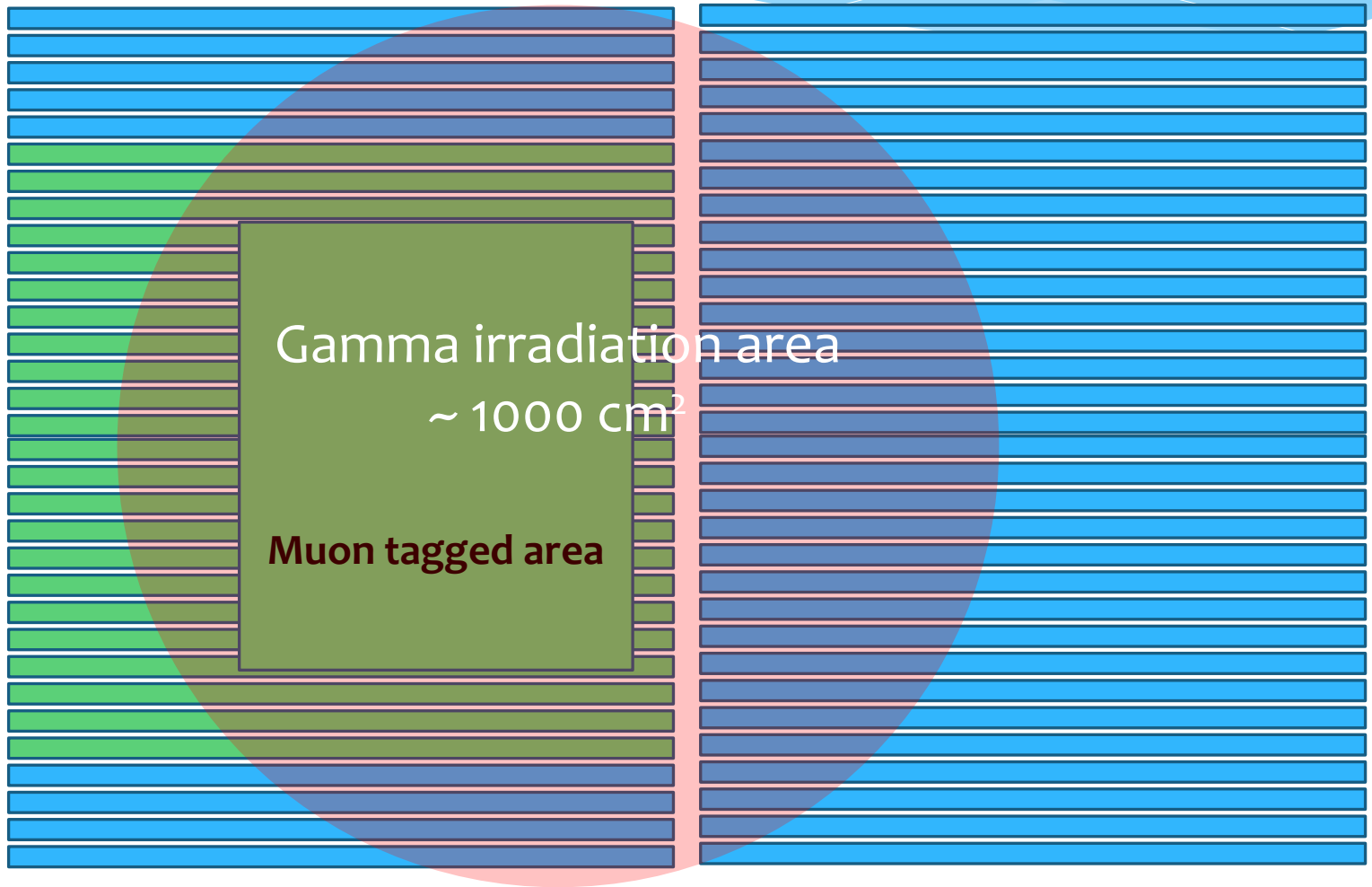


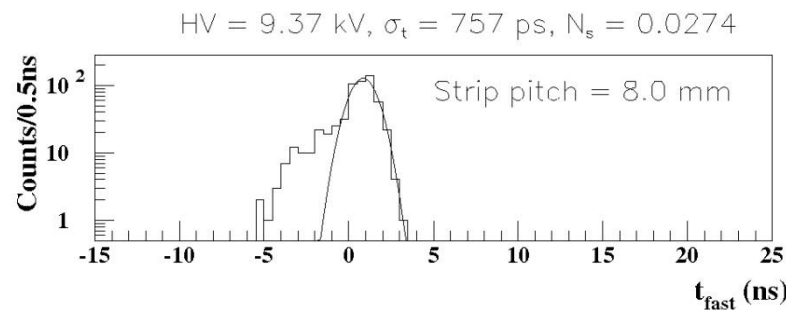
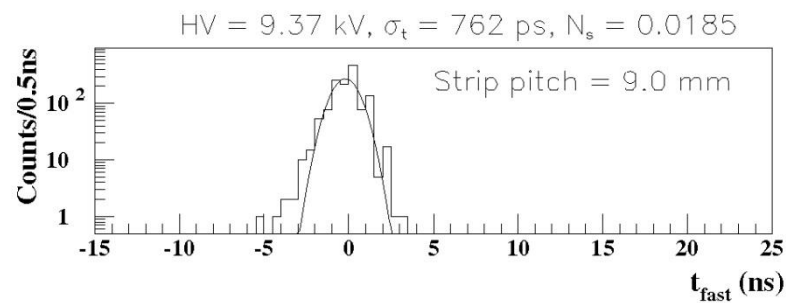
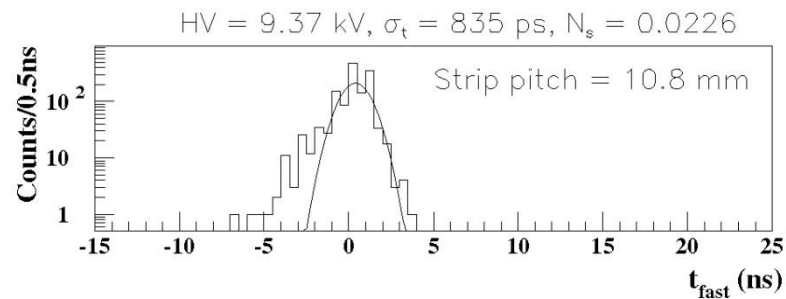
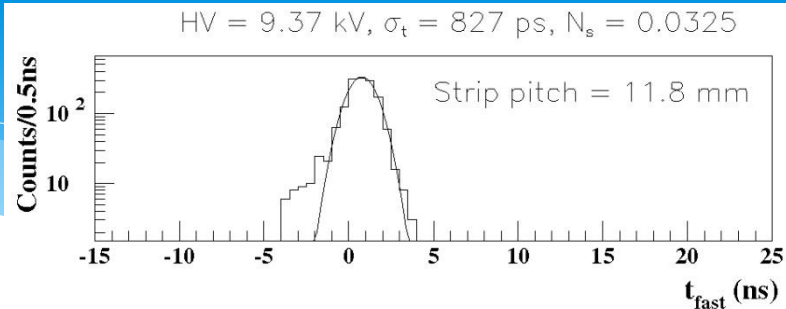
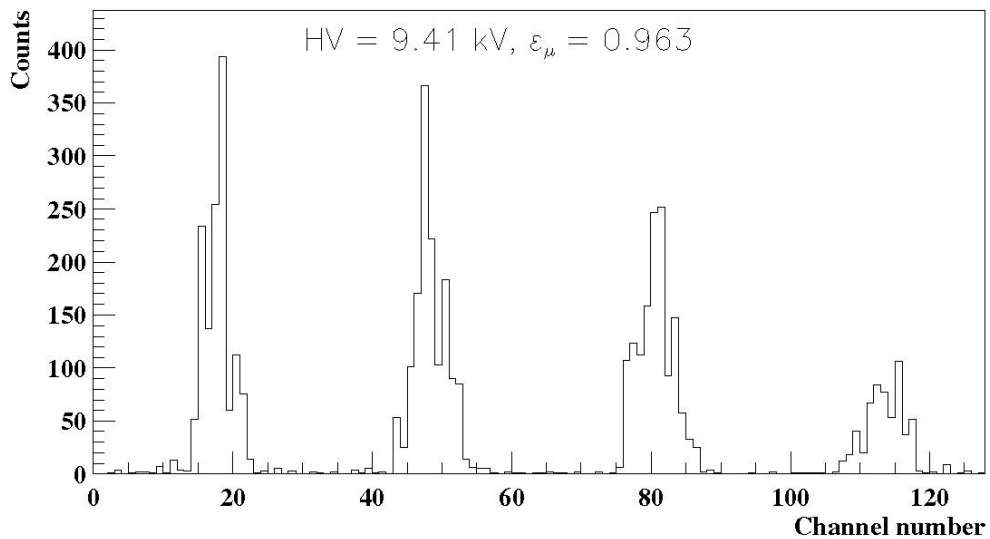
# Four-gap RPC





**Tagged muon hits in 16  $\mu$ s windows**  
**(from - 6  $\mu$ s to + 10  $\mu$ s centered at the muon peak)**  
**(strip area affected by gamma hits ~ 500 cm<sup>2</sup>)**





# Bulk resistivity of the HPL

Can be measured by applying gamma-ray signals with rates close to the detection capability limit (up to  $\sim 5 \text{ kHz cm}^{-2}$ )

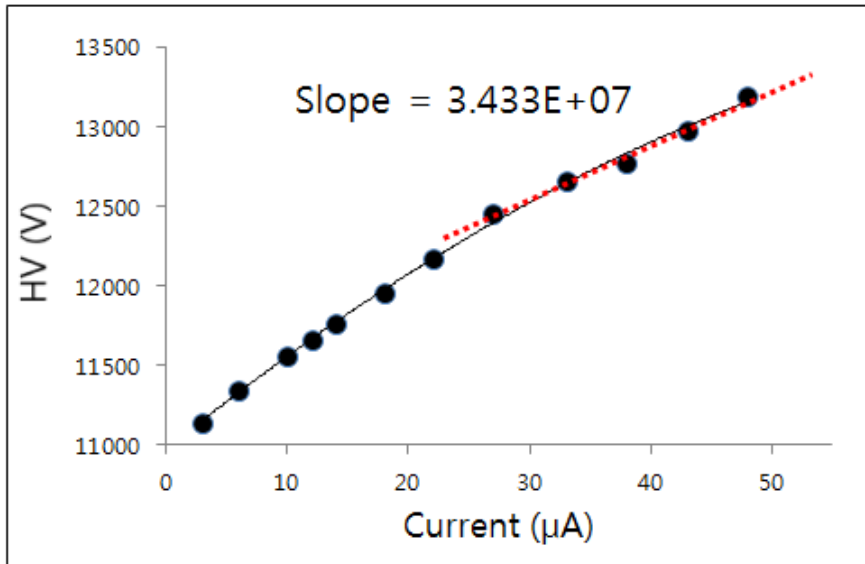
→ HV formed inside the gaps  $\sim$  insensitive to the increase of the applied HV

→  $\rho = (2.67 \pm 0.20) \times 10^{10} \Omega \text{ cm}$

Temperature coefficient  $\alpha = 0.13 \text{ }^\circ\text{C}^{-1}$

Irradiation area  $A \sim 500 \text{ cm}^2$ ,  $d = 6 \times 0.2 \text{ cm}$

$$\rho_b^{20} = \rho_T e^{\alpha(T-T_0)}$$



T = 24.97 C      P = 997.7 hPa      H = 73%

$$\Delta V = \rho * d/A \Delta I$$

| R          | A/d    | $\rho(24.79)$       | $\rho(20)$          |
|------------|--------|---------------------|---------------------|
| $\Omega$   | cm     | $\Omega \text{ cm}$ | $\Omega \text{ cm}$ |
| 3.433 E+07 | 416.67 | 1.4304 E+10         | 2.666 E+10          |

## Threshold dependence of cluster sizes (muon beam only)

Both double-gap and multi-gap RPCs: **shift < 100 V**.

LV 220 mV  $\Leftrightarrow$  170 fC

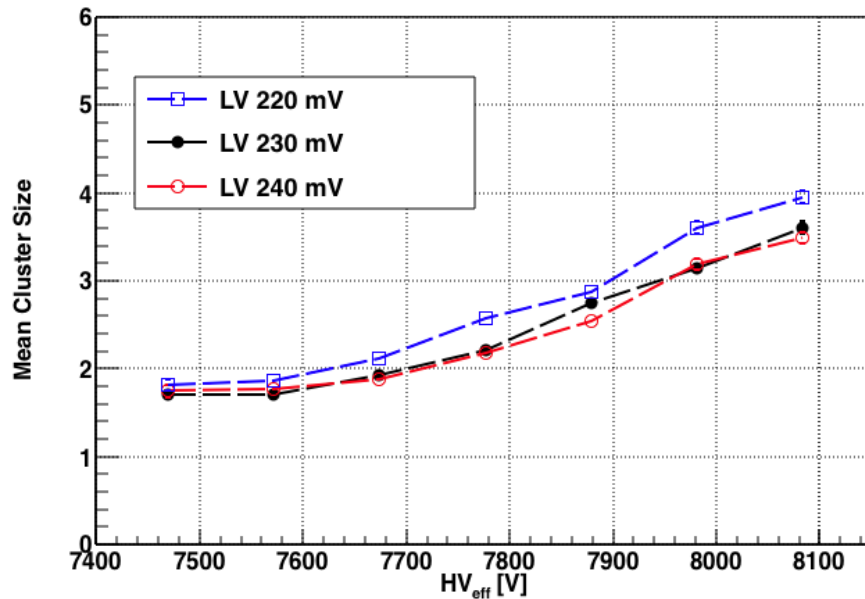
LV 230 mV  $\Leftrightarrow$  190 fC

LV 240 mV  $\Leftrightarrow$  240 fC

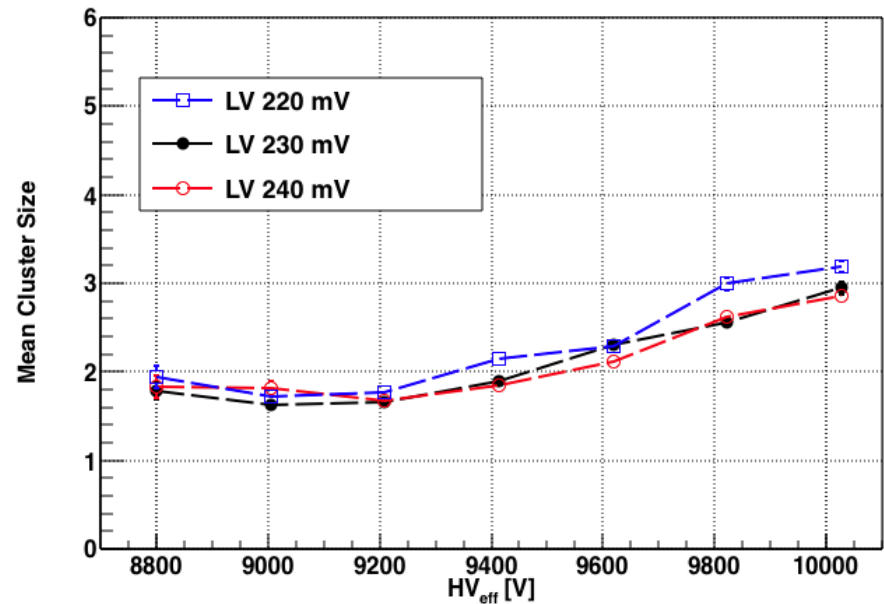
### Double-gap RPC

### Multi-gap RPC

KODEL Double-gap, Oct 2015 Test Beam, Att. 21.5



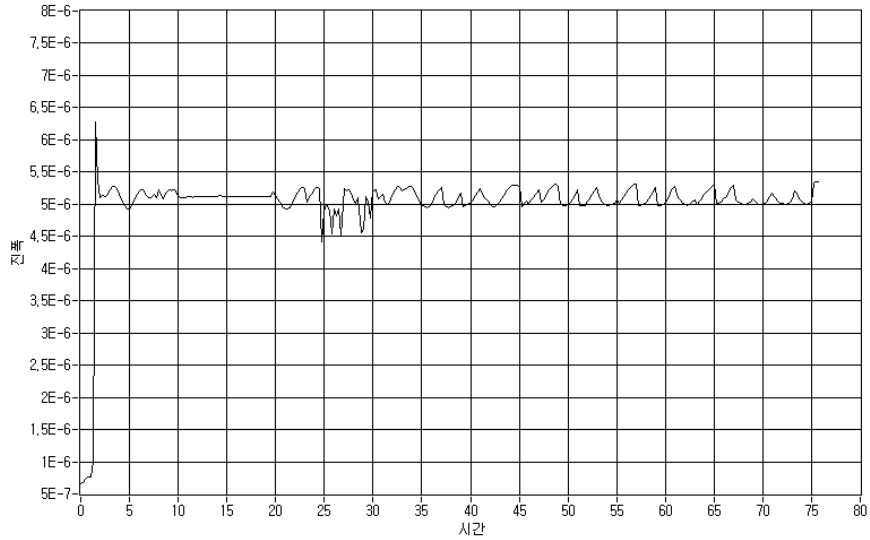
KODEL Multi-gap, Oct 2015 Test Beam, Att. 21.5



|                       |          |          |                          |         |          |          |                          |         |          |          |                          | 24.6/ 45%/<br>1009.3 |
|-----------------------|----------|----------|--------------------------|---------|----------|----------|--------------------------|---------|----------|----------|--------------------------|----------------------|
| HPL-resistivity value |          |          |                          | Current |          |          |                          | Current |          |          |                          |                      |
| N.O                   | average  | value    | DATA LINK                | N.O     | average  | value    | DATA LINK                | N.O     | average  | value    | DATA LINK                |                      |
| 1                     | 7.84E-06 | 2.56E+10 | <a href="#">01_graph</a> | 11      | 8.10E-06 | 2.48E+10 | <a href="#">11_graph</a> | 21      | 7.50E-06 | 2.68E+10 | <a href="#">21_graph</a> |                      |
| 2                     | 5.09E-06 | 3.95E+10 | <a href="#">02_graph</a> | 12      | 8.29E-06 | 2.43E+10 | <a href="#">12_graph</a> | 22      | 8.22E-06 | 2.45E+10 | <a href="#">22_graph</a> |                      |
| 3                     | 8.07E-06 | 2.49E+10 | <a href="#">03_graph</a> | 13      | 7.96E-06 | 2.53E+10 | <a href="#">13_graph</a> | 23      | 8.41E-06 | 2.39E+10 | <a href="#">23_graph</a> |                      |
| 4                     | 8.47E-06 | 2.37E+10 | <a href="#">04_graph</a> | 14      | 8.14E-06 | 2.47E+10 | <a href="#">14_graph</a> | 24      | 8.33E-06 | 2.41E+10 | <a href="#">24_graph</a> |                      |
| 5                     | 8.43E-06 | 2.38E+10 | <a href="#">05_graph</a> | 15      | 7.93E-06 | 2.53E+10 | <a href="#">15_graph</a> | 25      | 8.03E-06 | 2.50E+10 | <a href="#">25_graph</a> |                      |
| 6                     | 8.00E-06 | 2.51E+10 | <a href="#">06_graph</a> | 16      | 8.32E-06 | 2.42E+10 | <a href="#">16_graph</a> | 26      | 8.56E-06 | 2.35E+10 | <a href="#">26_graph</a> |                      |
| 7                     | 7.59E-06 | 2.65E+10 | <a href="#">07_graph</a> | 17      | 8.05E-06 | 2.50E+10 | <a href="#">17_graph</a> | 27      | 8.30E-06 | 2.42E+10 | <a href="#">27_graph</a> |                      |
| 8                     | 8.09E-06 | 2.48E+10 | <a href="#">08_graph</a> | 18      | 8.22E-06 | 2.45E+10 | <a href="#">18_graph</a> | 28      | 8.38E-06 | 2.40E+10 | <a href="#">28_graph</a> |                      |
| 9                     | 8.40E-06 | 2.39E+10 | <a href="#">09_graph</a> | 19      | 8.07E-06 | 2.49E+10 | <a href="#">19_graph</a> | 29      | 7.48E-06 | 2.69E+10 | <a href="#">29_graph</a> |                      |
| 10                    | 8.04E-06 | 2.50E+10 | <a href="#">10_graph</a> | 20      | 7.90E-06 | 2.55E+10 | <a href="#">20_graph</a> |         |          |          |                          |                      |

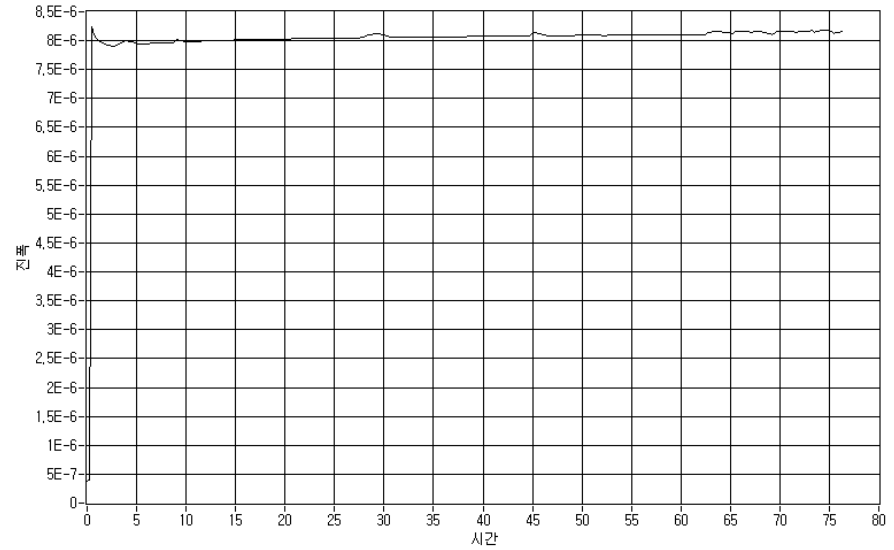


웨이브폼 그래프 2



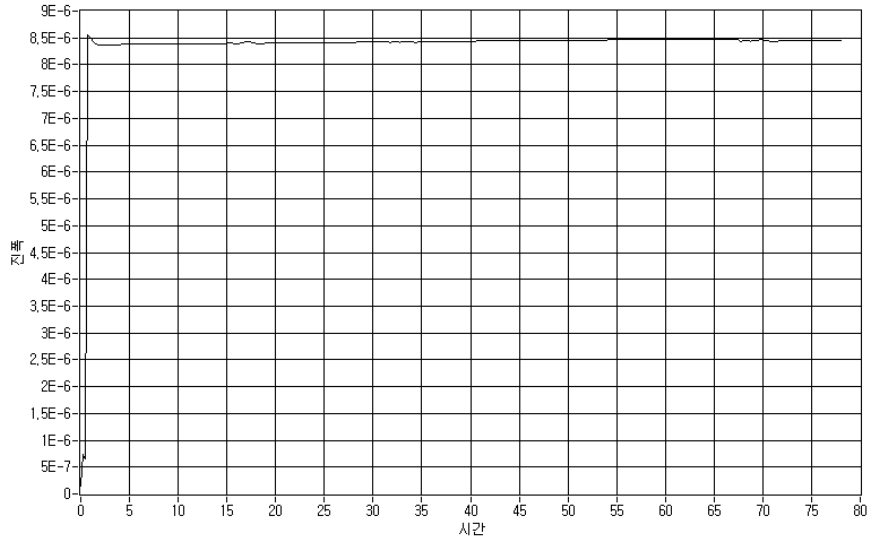
플롯 0

웨이브폼 그래프 2



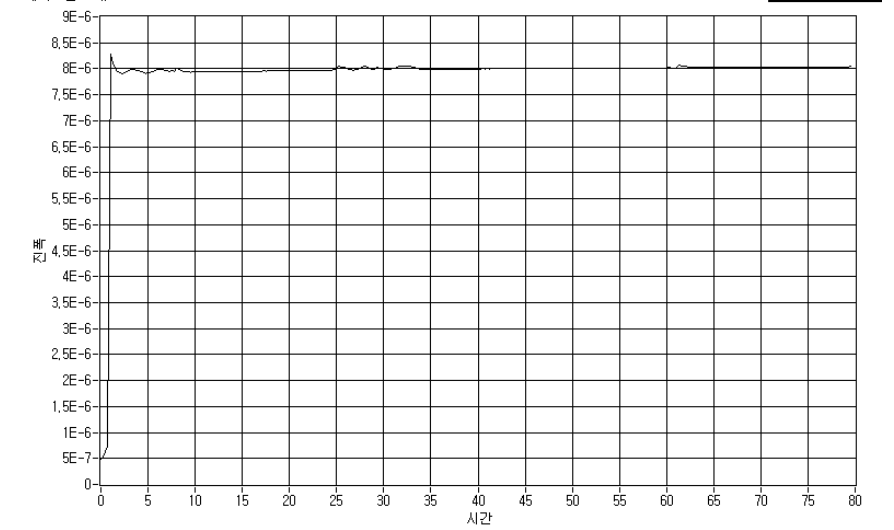
플롯 0

웨이브폼 그래프 2



플롯 0

웨이브폼 그래프 2



플롯 0